AD A023949

SDAC-TR-75-2

ADDITIONAL INVESTIGATION OF EARTHQUAKES WITH LOW M_s TO m_b RATIOS IN THE TIBET-HIMALAYA REGION

D. M. CLARK, E. I. SWEETSER and Z. A. DER

Seismic Data Analysis Center

Teledyne Geotech, 312 Montgomery Street, Alexandria, Virginia 22314

10 JULY 1975

APPROVED FOR PUBLIC RELEASE; DISTRIBUTION UNLIMITED.

Sponsored By

The Defense Advanced Research Projects Agency

Nuclear Monitoring Research Office

1400 Wilson Boulevard, Arlington, Virginia 22209

ARPA Order No. 1620

Monitored By

VELA Seismological Center

312 Montgomery Street, Alexandria, Virginia 22314

DDC

RECEIVED

MAY 5 1976

B

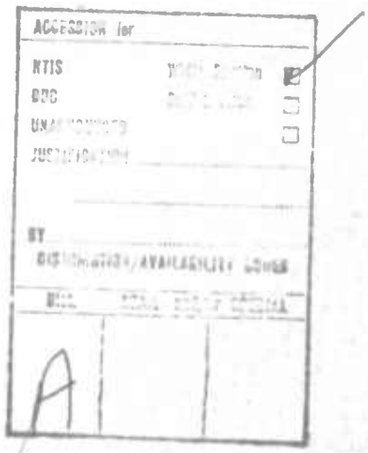

Disclaimer: Neither the Defense Advanced Research Projects Agency nor the Air Force Technical Applications Center will be responsible for information contained herein which has been supplied by other organizations or contractors, and this document is subject to later revision as may be necessary. The views and conclusions presented are those of the authors and should not be interpreted as necessarily representing the official policies, either expressed or implied, of the Defense Advanced Research Projects Agency, the Air Force Technical Applications Center, or the US Government.

Unclassified

SECURITY CLASSIFICATION OF THIS PAGE (When Data Entered)

REPORT DOCUMENTATION PAGE

READ INSTRUCTIONS BEFORE COMPLETING FORM

1. REPORT NUMBER: SDAC-TR-75-2
2. GOVT ACCESSION NO.
3. RECIPIENT'S CATALOG NUMBER

4. TITLE (and Subtitle): ADDITIONAL INVESTIGATION OF EARTHQUAKES WITH LOW M_s TO m_b RATIOS IN THE TIBET-HIMALAYA REGION.
5. TYPE OF REPORT & PERIOD COVERED: Technical rept.
6. PERFORMING ORG. REPORT NUMBER

7. AUTHOR(s): Clark, D. M.; Sweetser, E. I.; Der, Z. A.
8. CONTRACT OR GRANT NUMBER(s): F08606-76-C-0004; ARPA Order-1620

9. PERFORMING ORGANIZATION NAME AND ADDRESS: Teledyne Geotech, 314 Montgomery Street, Alexandria, Virginia 22314
10. PROGRAM ELEMENT, PROJECT, TASK AREA & WORK UNIT NUMBERS: VT/6709

11. CONTROLLING OFFICE NAME AND ADDRESS: Defense Advanced Research Projects Agency, Nuclear Monitoring Research Office, 1400 Wilson Blvd.-Arlington, Virginia 22209
12. REPORT DATE: 10 July 1975
13. NUMBER OF PAGES: 67

14. MONITORING AGENCY NAME & ADDRESS (if different from Controlling Office): VELA Seismological Center, 312 Montgomery Street, Alexandria, Virginia 22314
15. SECURITY CLASS. (of this report): Unclassified
15a. DECLASSIFICATION DOWNGRADING SCHEDULE

16. DISTRIBUTION STATEMENT (of this Report):

APPROVED FOR PUBLIC RELEASE; DISTRIBUTION UNLIMITED.

17. DISTRIBUTION STATEMENT (of the abstract entered in Block 20, if different from Report)

D. M. Clark, E. I. Sweetser Zoltan A. Der

18. SUPPLEMENTARY NOTES

19. KEY WORDS (Continue on reverse side if necessary and identify by block number)

Discriminants
M_s-m_b
Anomalous Events

20. ABSTRACT (Continue on reverse side if necessary and identify by block number)

Further analysis of the anomalous events in the eastern Himalaya region with an expanded set of stations shows that the M_s values of these events are indeed low compared to m_b. Other characteristics of these events indicate, however, that all these events are earthquakes rather than explosions. Dilatational first motion for P waves, long period S to Rayleigh, short period S to P wave amplitude ratios are characteristic of earthquakes. Readings of the pP phase where available as well as epicenter calculations

(cont on R 1473 B)

DD FORM 1 JAN 73 1473 EDITION OF 1 NOV 65 IS OBSOLETE

Unclassified

SECURITY CLASSIFICATION OF THIS PAGE (When Data Entered)

408 258 LB

(M sub s - m sub b

(cont'd fr 1473A)

indicate that the anomalous event hypocenter are shallow, i.e., less than 80 km. Data quality did not permit the refinement of epicenter locations.

A search for additional anomalous events with respect to $(M_s - m_b)$ in a wider area in the Himalayan-Tibet region indicated that there are no other contiguous areas containing anomalous events in this region beyond those already found.

1473B

ADDITIONAL INVESTIGATION OF EARTHQUAKES WITH LOW M_s TO m_b RATIOS IN THE TIBET-HIMALAYA REGION

SEISMIC DATA ANALYSIS CENTER REPORT NO.: SDAC-TR-75-2

AFTAC Project Authorization No.:	VELA T/6709/B/ETR
Project Title:	Seismic Data Analysis Center
ARPA Order No.:	2551
ARPA Program Code No.:	6F10
Name of Contractor:	TELEDYNE GEOTECH
Contract No.:	F08606-76-C-0004
Date of Contract:	01 July 1975
Amount of Contract:	$2,319,926
Contract Expiration Date:	30 June 1976
Project Manager:	Royal A. Hartenberger (703) 836-3882

P. O. Box 334, Alexandria, Virginia 22314

APPROVED FOR PUBLIC RELEASE; DISTRIBUTION UNLIMITED.

ABSTRACT

Further analysis of the anomalous events in the eastern Himalaya region with an expanded set of stations shows that the M_s values of these events are indeed low compared to m_b. Other characteristics of these events indicate, however, that all these events are earthquakes rather than explosions. Dilatational first motion for P waves, long period S to Rayleigh, short period S to P wave amplitude ratios are characteristic of earthquakes. Readings of the pP phase where available as well as epicenter calculations indicate that the anomalous event hypocenter are shallow, i.e., less than 80 km. Data quality did not permit the refinement of epicenter locations.

A search for additional anomalous events with respect to M_s-m_b in a wider area in the Himalayan-Tibet region indicated that there are no other contiguous areas containing anomalous events in this region beyond those already found.

TABLE OF CONTENTS

LIST OF FIGURES

LIST OF FIGURES (Continued)

LIST OF TABLES

INTRODUCTION

This report is a supplement to a previous report on low M_s events in the Himalayan region (Der, 1973), hereafter referred to as Report #296. It includes additional data for a larger network of stations, an evaluation of discriminants other than M_s vs. m_b, and a search for low M_s events.

We first reanalyze the anomalous events from 296 with respect to depth as determined from P and S-P times, and from P-pP times. Discrimination by means of short-period S to P amplitude ratios is discussed, and the possible use of LQ/LR ratios is explored. Then the effects on M_s-m_b values of more complete P wave data is explored together with the expected effects on M_s of an abnormally thick crust. Finally we report on the use of station KBL to search for anomalous events in a wider area than searched in SDL 296.

DATA

The events selected from Report #296 for this study are shown in Table I. Two criteria were used in the selection: the low M_s value compared to m_b, and the proximity of the epicenter to 30°N and 95°E regardless of relative $M_s - m_b$ values, although most of the 30°N, 95°E events also qualify as "low M_s" earthquakes.

In addition to the station network used in the previous study (Der, 1973) we acquired data from the WWSSN stations AAE, BUL, CTA, COL, SEO, TRI and NUR. The map on Figure 1 shows the location of all the stations used. The basic data consists of short and long period seismograms on 35 mm film chips. The quality of recordings is often poor, and the quality of stations is often very unequal. Some operate at high gains and are very useful (KBL for example) while some (LAH for example) are almost useless. Most of the recordings are not suitable for digital conversion because of the poor data quality.

TABLE I

LIST OF EVENTS STUDIED

	Yr	Mo	Day	Hr	Min	Sec	Coordinates N. Lat	Coordinates E. Long	SDL 296 M_s	SDL 296 m_b	New Avg. m_b	Depth
1	64	10	06	2	54	32.7	30.3	94.6	3.61	-	4.54	N*
2	66	07	05	10	1	22.0	27.5	92.4	3.90	5.32	5.32	77
3	66	09	11	15	55	20.0	27.0	95.8	3.77	5.24	4.69	37
4	66	09	26	6	3	48.0	27.6	92.7	3.59	4.49	5.39	N
5	67	07	07	22	56	30.8	27.8	92.2	3.71	4.76	4.78	N
6	68	06	28	20	34	55.3	30.1	95.1	3.54	4.77	4.82	44
7	68	06	30	5	4	10.0	30.2	94.8	3.40	4.61	4.64	42
8	68	07	01	3	11	10.0	30.3	94.5	3.00	4.14	4.40	28
9	68	07	04	6	45	58.0	30.3	94.9	3.46	4.87	4.82	N
10	68	07	13	6	5	54.2	30.3	94.6	3.46	4.73	4.75	N
11	68	07	14	18	12	41.0	30.3	94.8	3.54	4.72	4.89	22
12	68	07	16	22	23	7.0	30.3	94.8	3.45	4.57	4.70	40
13	68	07	19	18	48	59.0	30.2	94.9	3.56	-	4.80	N
14	68	07	23	20	51	47.9	30.3	94.9	3.43	4.57	4.69	30
15	68	07	25	3	34	13.0	30.2	94.8	3.27	-	4.90	N
16	68	07	26	12	44	3.0	29.4	95.0	3.45	4.65	4.73	N
17	68	08	23	12	1	16.5	30.3	94.9	3.46	4.62	4.75	N
18	68	08	25	17	55	5.3	30.4	94.8	3.28	4.39	4.58	19
19	68	08	29	19	51	24.6	30.2	95.1	3.48	4.55	4.68	N
20	68	09	01	5	59	26.6	30.3	94.8	3.59	4.56	4.60	20
21	68	09	03	17	45	54.1	30.2	94.8	3.43	4.52	4.64	53
22	69	08	15	7	15	37.0	30.2	95.0	3.57	4.87	4.90	N

N = normal depth ~33 km

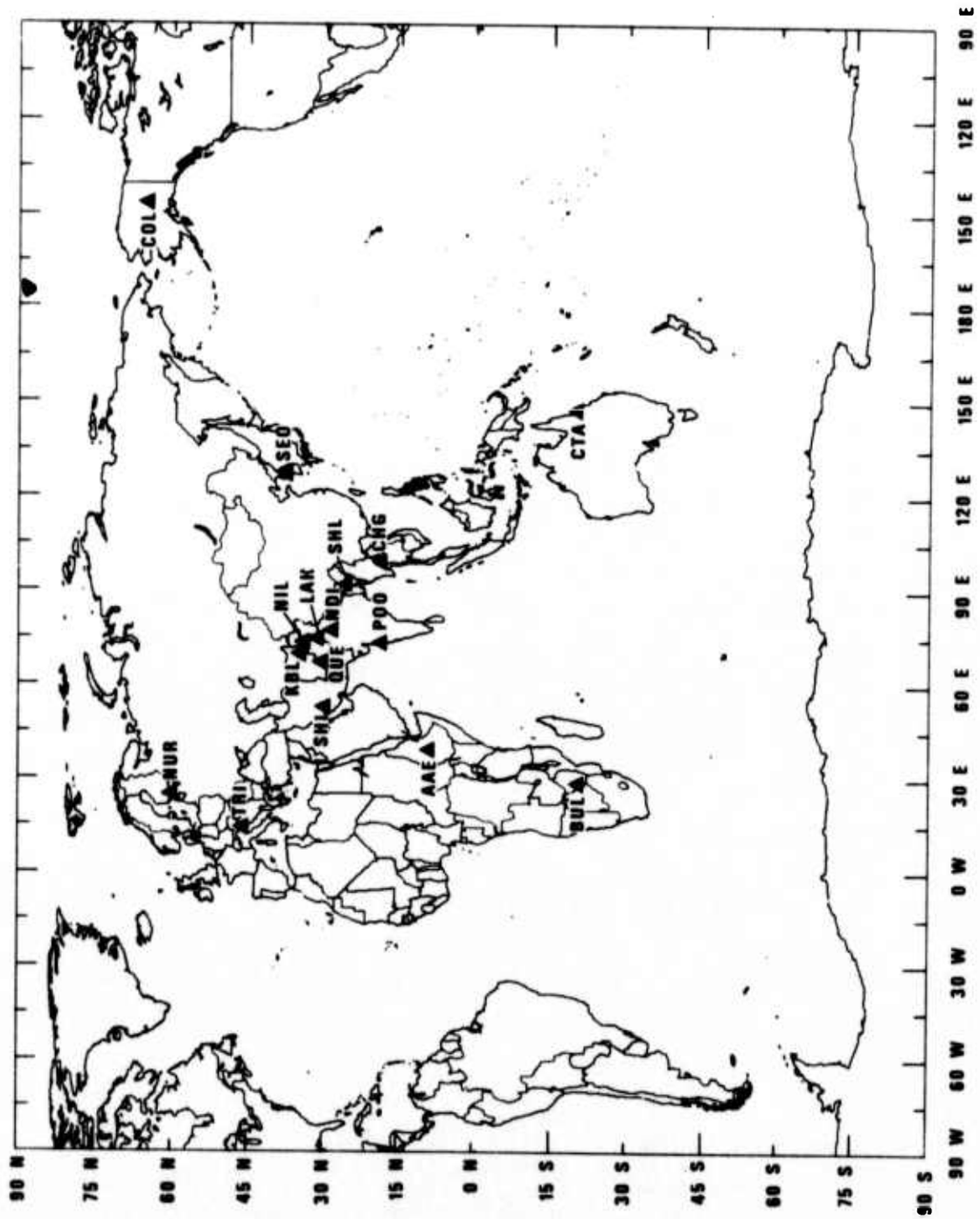

Figure 1. Map of the area studied and the seismic stations used.

RESULTS OF DATA ANALYSIS

SHORT-PERIOD WAVE TRAVEL TIMES

Table II shows the arrival times of short period P and S waves read from the film chips. Arrival times with estimated uncertainties larger than 3 sec were omitted from the table.

P WAVE FIRST MOTIONS

No clear long-period P waves were found for the clustered events, but short-period P wave first motions have been observed for many of the events. The readings and their quality classifications are given in Table III. Single events do not have enough readings to define a fault plane solution. Nevertheless clear dilatations have been observed (Figure 2a). We considered the possibility that the events clustered at 35°N, 95°E could possess a common source mechanism as many earthquake swarms and aftershock sequences do. The combined first motions, however, for the event cluster do not show a pattern consistent with any common fault plane solution. The presence of dilatations indicates, however, that the events in question are earthquakes and not explosions.

SHORT-PERIOD WAVE AMPLITUDES

Table IV shows the amplitudes and dominant periods of short period P and S waves at stations where both types of waves could be observed. Von Seggern (1972) showed that the ratio of the amplitudes of short-period P and S waves is a discriminant between earthquakes and explosions. The ratios in Table IV are characteristic of earthquakes as seen by comparison with Figure 2b taken from the report by von Seggern.

pP PHASES

The pP-P times read at teleseismic stations are shown in Table V. The pP phases are uncertain and the times do not have the proper moveout for pP phases, this indicates that some of the phases were incorrectly identified. The depth range consistent with the pP-P times are also given in the table. All the depths are shallow, and are not inconsistent with National Ocean Survey (NOS) depths in Table I.

TABLE II

Travel Times of P and S Waves

No.	Event Date/Time	Station	P-Time	S-Time	Component
1	64/10/06 t=02:54:33.0	CHG	02:57:24.7		
		COL	03:06:03.5		
		NDI	02:58:08.0		
		SHI	03:01:30.6		
		SHL	02:55:52.0		
		TRI	03:04:55.3		
2	66/07/05 t=10:01:22.0	NDI	10:04:28.8	10:06:55.0	
		QUE	10:06:19.0	10:10:33.6	
		SHL	10:01:55.2		
3	66/07/05 t=15:55:20	NDI	16:07:30.0		
		CHG	15:57:29.5	15:57:29.5	
		COL	16:07:05.0		
		NDI	15:59:04.5	16:01:55.2	
		NUR	16:05:05.0		
		SEO	16:01:09.3		
		SHI	16:02:35.2		
		SHL	15:56:18.0		
4	66/09/26	CHG	06:06:17.3		
		COL	06:15:39.0		
		NDI	06:07:00.7		
		POO	06:08:16.0		
		QUE	06:08:50.0		
		SHL	06:04:23.3		
5	67/07/07 t=22:56:30.8	BUL	23:08:28.2		
		CHG	22:49:06.5		
		COL	23:08:22.0		
		NDI	22:59:30.6	23:01:51.0	
		QUE	23:01:25.7	23:05:41.0	
		SHI	23:03:19.0		
		TRI	23:06:54.5		
6	68/06/28 t=20:34:55	BUL	20:47:08.0		
		CHG	20:37:47.0		
		COL	20:46:25.2		
		CTA	20:46:03.0		
		KBL	20:39:49.2	20:43:53.0	SPE
		QUE	20:40:10.5		
		SHL	20:36:14.9		
		TRI	20:45:20.0		

TABLE II (Continued)

Travel Times of P and S Waves

No.	Event Date/Time	Station	P-Time	S-Time	Component
7	68/06/30	BUL	05:16:22.8		
	t=05:04:10.0	CHG	05:07:02.6		
		COL	05:15:39.5		
		KBL	05:09:04.1	05:13:08.1	SPN
		SHL	05:05:30.0	05:06:21.5	
8	68/07/01	BUL	03:23:20.0		
	t=03:11:10.0	CHG	03:14:02.7		
		COL	03:22:37.0		
		SHL	03:12:28.9	03:13:26.0	SPN
9	68/07/04	BUL	06:58:11.0		
	t=06:45:58.0	COL	06:57:29.0		
		KBL	06:50:52.3	06:54:56.1	SPN
		NUR	06:55:21.0		
		SHI	06:53:02.9		
10	68/07/13	BUL	06:18:05.0		
		CHG	06:08:45.8		
		COL	06:17:22.5		
		CTA	06:17:07.2		
		KBL	06:10:47.6	06:14:51.0	SPE
		NDI	06:09:26.2		
		NUR	06:15:19.5		
		QUE	06:11:04.5		
		SHI	06:12:56.5		
		TRI	06:16:17.0		
11	68/07/14	BUL	18:24:56.2		
	t=18:21:41	CHG	18:15:35.3		
		COL	18:24:11.0		
		KBL	18:17:36.4	18:21:40.1	SPE
		NDI	18:16:15.5		
		NUR	18:22:07.5		
		POO	18:17:40.0		
		SHI	18:19:45.5		
		SHL	18:14:02.8		
		TRI	18:23:08.5		
12	68/07/16	BUL	22:34:19.5		
	t=22:23:07.0	CHG	22:25:56.2		
		COL	22:34:36.0		
		CTA	22:34:17.4		
		KBL	22:28:00.9	22:32:04.0	SPN

TABLE II (Continued)

Travel Times of P and S Waves

No.	Event Date/Time	Station	P-Time	S-Time	Component
		NDI	22:26:39.3		
		NUR	22:32:32.2		
		SHI	22:30:09.9		
		SHL	22:24:26.9		
13	68/07/19 t=18:48:59	AAE	18:58:41.5		
		BUL	19:01:11.9		
		CHG	18:51:51.8		
		COL	19:00:30.7		
		KBL	18:53:54.5	18:57:57.0	SPN
		NDI	18:52:32.4		
		NUR	18:58:25.9		
		QUE	18:54:12.8	18:58:33.0	SPN
		SHI	18:56:03.0		
		SHL	18:50:19.5		
		TRI	18:59:24.9		
14	68/07/23	BUL	21:04:02.0		
		CHG	20:54:41.0		
		COL	21:03:18.5		
		KBL	20:56:43.4	21:00:46.4	SPN
		NDI	20:55:21.5		
		NUR	21:01:13.0		
		SHL	20:53:08.5		
		SHI	20:58:50.8		
15	68/07/25 t=03:34:13	BUL	03:46:25.5		
		CHG	03:37:06.2		
		COL	03:45:43.0		
		NDI	03:37:46.8		
		NUR	03:43:37.0		
		SHI	03:41:15.5		
16	68/07/26 t=12:44:03	AAE	12:53:44.0		
		BUL	12:56:14.5		
		CHG	12:46:59.5		
		COL	12:55:37.9		
		CTA	12:55:15.0		
		KBL	12:49:02.0	12:53:05.0	SPE
		NUR	12:53:33.5		
		QUE	12:49:23.3		
		SHI	12:51:11.0		
		SHL	12:45:12.7	12:46:12.5	SPE
		TRI	12:54:38.0		

TABLE II (Continued)

Travel Times of P and S Waves

No.	Event Date/Time	Station	P-Time	S-Time	Component
17	68/08/23 t=12:01:16	BUL	12:13:34.5		
		CHG	12:04:07.7		
		COL	12:12:45.0		
		CTA	12:12:31.8		
		KBL	12:06:10.7	12:10:14.1	SPN
		NDI	12:04:50.0		
		NUR	12:10:42.5		
		QUE	12:06:35.7		
		SHL	12:02:37.0	12:03:34.2	SPE
18	68/08/25 t=17:55:05	BUL	18:07:20.0		
		CHG	17:57:59.4		
		COL	18:06:38.0		
		CTA	18:06:19.3		
		KBL	18:00:01.4	18:04:04.5	SPE
		NDI	17:58:41.1		
		NUR	18:04:33.0		
		QUE	18:00:20.2		
		SHL	17:56:27.5	17:57:36.7	SPE
19	68/08/29 t=19:51:25	BUL	20:03:37.5		
		CHG	19:54:17.3		
		COL	20:02:55.0		
		CTA	20:02:35.0		
		KBL	19:56:19.0	20:00:22.8	SPN
		NDI	19:54:59.4		
		NUR	20:00:49.7		
		SHI	19:58:28.8		
		SHL	19:52:45.0		
		TRI	20:01:50.0		
20	68/09/01 t=05:59:27	BUL	06:11:41.5		
		CHG	06:02:19.5	06:08:26.0	SPN
		COL	06:10:59.0		
		CTA	06:10:37.9		
		KBL	06:06:06.0		
		SHI	06:06:32.0		
		SHL	06:00:48.4		
21	68/09/03 t=17:45:54	CHG	17:48:45.0		
		COL	17:57:22.0		
		CTA	17:57:03.0		
		KBL	17:50:47.2	17:54:50.5	SPE

TABLE II (Continued)

Travel Times of P and S Waves

No.	Event Date/Time	Station	P-Time	S-Time	Component
		NDI	17:49:26.0		
		NUR	17:55:16.5		
		POO	17:50:49.3		
		QUE	17:51:08.7		
		SHL	17:47:12.1	17:48:08.0	SPN
22	69/08/15 t=07:15:37	CHG	07:18:42.8		
		COL	07:27:07.9		
		KBL	07:20:32.7	07:24:37.0	
		NIL	07:19:51.6	07:23:27.0	
		QUE	07:20:52.5		
		SHI	07:22:42.0		
		SHL	07:16:57.4	07:17:51.7	

TABLE III

First Motions

No.	1	6	7	8	9	10	11	12	13	14	15	16	17	18
	10/6	6/28	6/30	7/01	7/04	7/13	7/14	7/16	7/19	7/23	7/25	7/26	8/23	8/25
	64	68	68	68	68	68	68	68	68	68	68	68	68	68
SHL	-	-	+	+			-	+	-?	-?		+?	-	-
QUE		+?	+?	+?	+?	+?	+?	+?	+	+?	-?	+?	+?	+?
POO							-?							
NDI	+?					-?	+?	+?	-	+?	-?			+?
LAH														
KBL		+	-		+	+	+	-	-?	-			+	-
CHG	-?	-	?	+?		+	+	+?	-	+	-?	+	-?	+?

+ Up

- Down

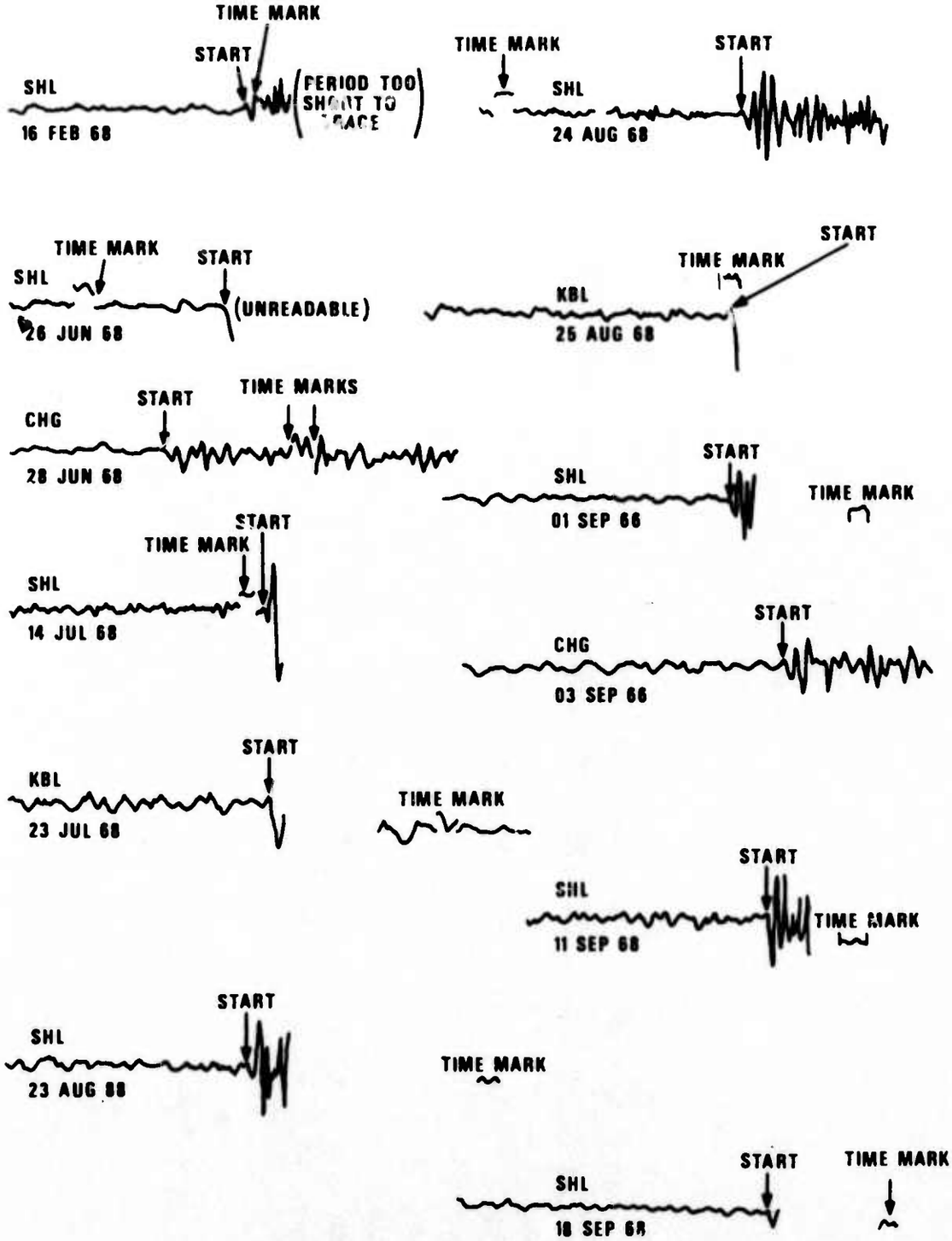

Figure 2a. Dilatational first motion observed for various events.

TABLE IV

Short Period S/P Amplitude Ratios

Event	Station	R(S/P Amplitude Ratio)	Log R
7/05/66	QUE	1.4	0.16
	NDI	28.4	1.45
7/07/67	QUE	5.5	0.74
	NDI	29.7	1.47
6/28/68	KBL	1.3	0.10
6/30/68	CHG	2.6	0.41
	SHL	16.0	1.20
	KBL	0.4	-0.45
7/01/68	SHL	77.1	1.89
7/26/68	KBL	1.1	0.05
	SHL	65.4	1.82
8/23/68	SHL	31.1	1.49
8/25/68	SHL	1.1	0.06
8/29/68	SHL	0.8	-0.11
9/03/68	SHL	15.0	1.18
8/15/69	SHL	7.8	0.89

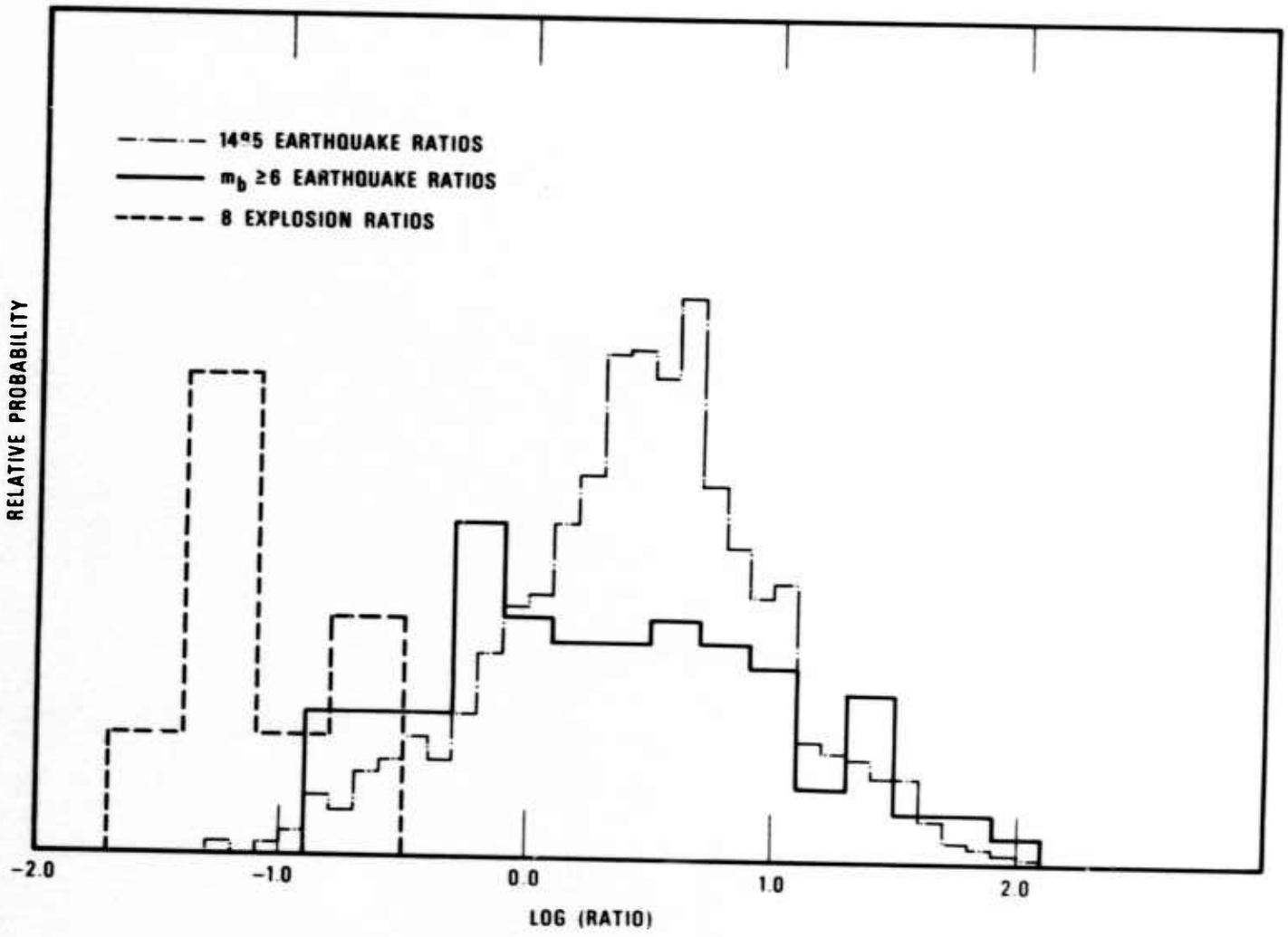

Figure 2b. Ratios of short-period S to short-period P displacement for worldwide earthquakes and underground nuclear explosions in Nevada and on Amchitka Island. (After von Seggern, 1972)

TABLE V

pP - P Times

	SEQ	SHI	NUR	AAE	CTA	COL	BUL	TRI	Avg DEPTH(km)
66/09/11	-	-	-	-	-	6.0	-	-	20
67/07/07	-	5.5	-	-	-	+	+	+	17
68/06/28	-	-	-	-	5.5	+	+	+	17
68/07/01	-	NR	NR	-	-	5.0	+	-	16
68/07/13	-	4.6	+	-	+	7.5	+	2.5	10-24
68/07/14	?	5.0	5.0	-	-	6.5	+	11.5	17-40
68/07/16	-	10.1	+	-	+	9.5	+	-	~35
68/07/23	-	7.4	?	-	-	+	5.9	-	15-27
68/07/25	-	9.5	+	-	-	+	+	-	35-40
68/07/26	-	10.5?	+	+	5.0	+	+	4.5	14-15
68/08/25	-	NR	5.0	-	4.2	+	+	-	13-18
68/08/29	-	7.9	+	-	+	+	5.0	+	15-27
68/09/01	?	+	-	-	+	+	4.5	?	12
69/08/15	-	+	?	-	-	10.1	-	-	33

\+ P Observed, no pP

\- No P

NR No Record

? Doubtful Readings

DESCRIPTION OF LONG-PERIOD SEISMOGRAMS

Events Clustered at 30°N and 95°E

Figures 3 through 9 show long-period three-component seismograms at Shillong (SHL) for seven events. SHL is the only station which recorded the surface waves well from the event cluster at 30°N, 95°E. Weak surface waves were observed at other stations, especially at Chiang Mai (CHG), but these are hardly worth reproducing due to the low signal-to-noise ratio. The recordings at Shillong all show a Rayleigh pulse on the vertical component which remains reasonably similar from event to event. The group velocity of the Rayleigh pulse is about 3km/sec and the period is about 10 sec. The horizontal components are also very similar from event to event to a very fine level of detail. Short-period waves corresponding to Lg arrive before the Rayleigh pulse and there are indications of longer period waves, probably fundamental Love, preceding the Rayleigh pulse.

The Rayleigh pulse is also seen on the horizontal components. The ratio of the horizontal to vertical amplitude is close to .7 ruling out the possibility of the pulse consisting of higher modes since for higher modes this ratio should be much lower for any reasonable mantle structure. The waveforms are quite similar, suggesting similar source mechanisms for these events.

Discussion of Long-Period Seismograms of Events not Located at 30°N, 95°E

The most prominent feature of long-period seismograms from the 10/06/64 event is the Rayleigh wave (Figure 10). Higher mode surface waves may be also present in the higher frequency waves preceding the Rayleigh pulse. The quality of seismograms is poor.

Figure 11 shows seismograms of the event 7/05/66 recorded at Shillong at a distance of 220 km. P and S phases are visible. There is an indication of Love waves. The depth of this event was given by the NOS as 77 km.

Figure 12 shows seismograms for the event 9/11/66. At Shillong long-period P and S phases are faintly visible. Clear Rayleigh and Love waves are present. There are indications of higher Rayleigh modes in the form of short-period waves preceding the fundamental Rayleigh mode on the vertical component.

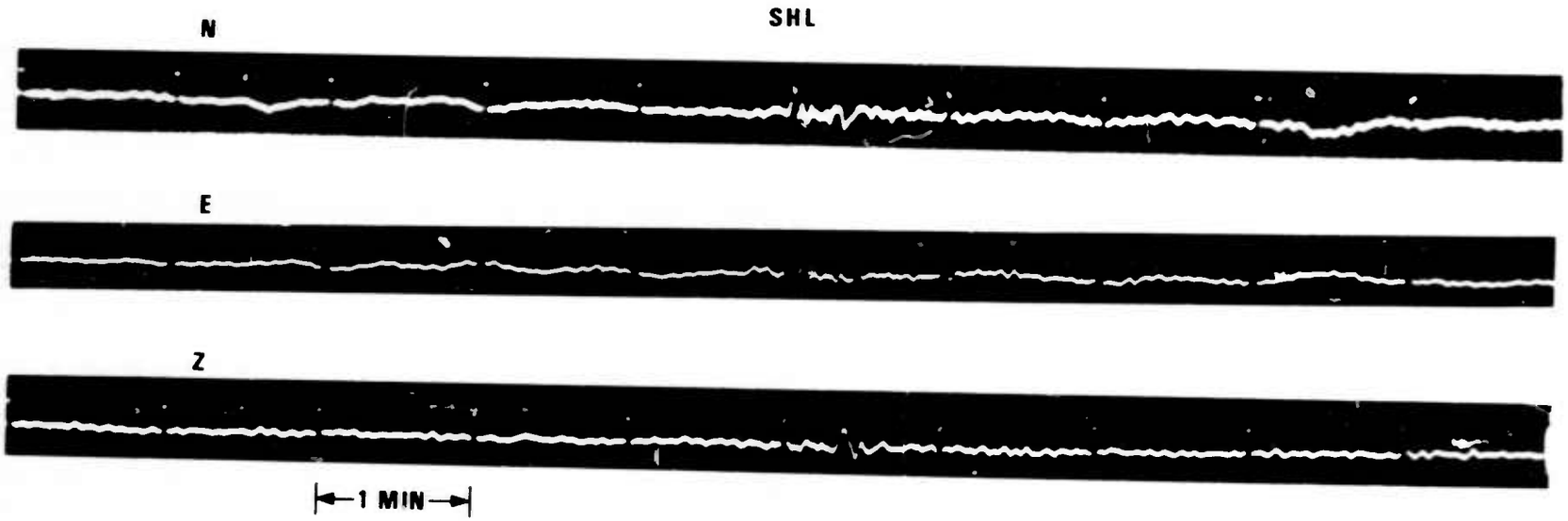

Figure 3. Long-period seismograms for the event on 7/04/68, 30.3°N 94.9°E, recorded at SHL.

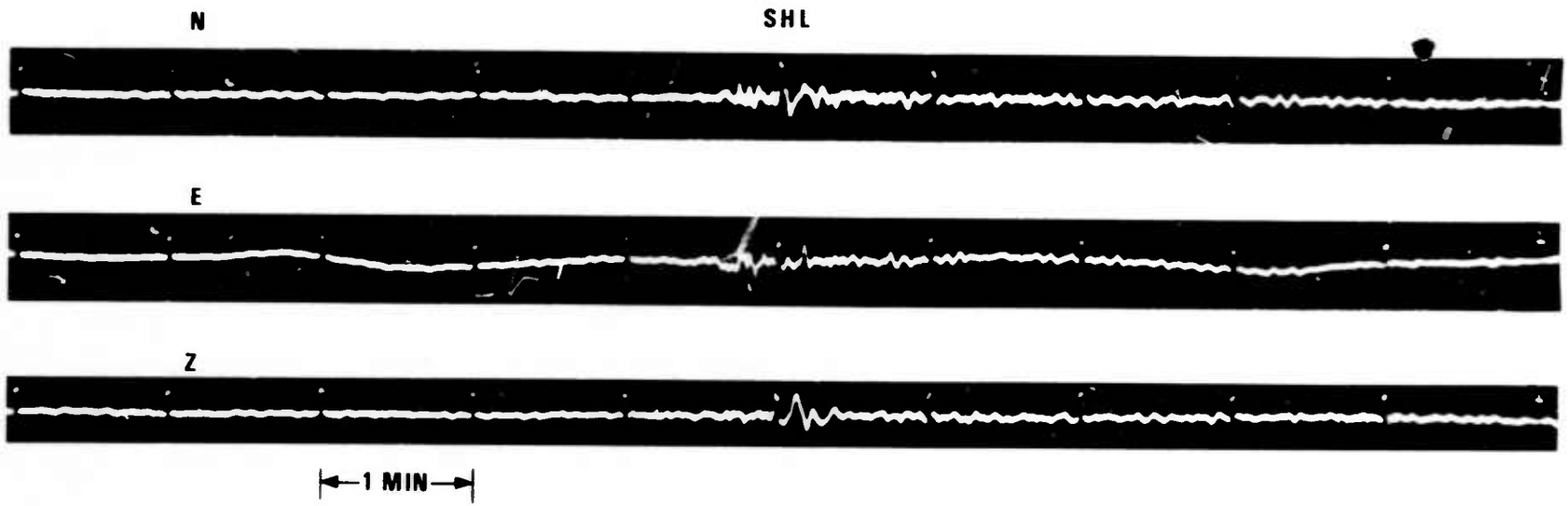

Figure 4. Long-period seismograms for the event on 7/14/68, 30.3°N 94.8°E, recorded at SHL.

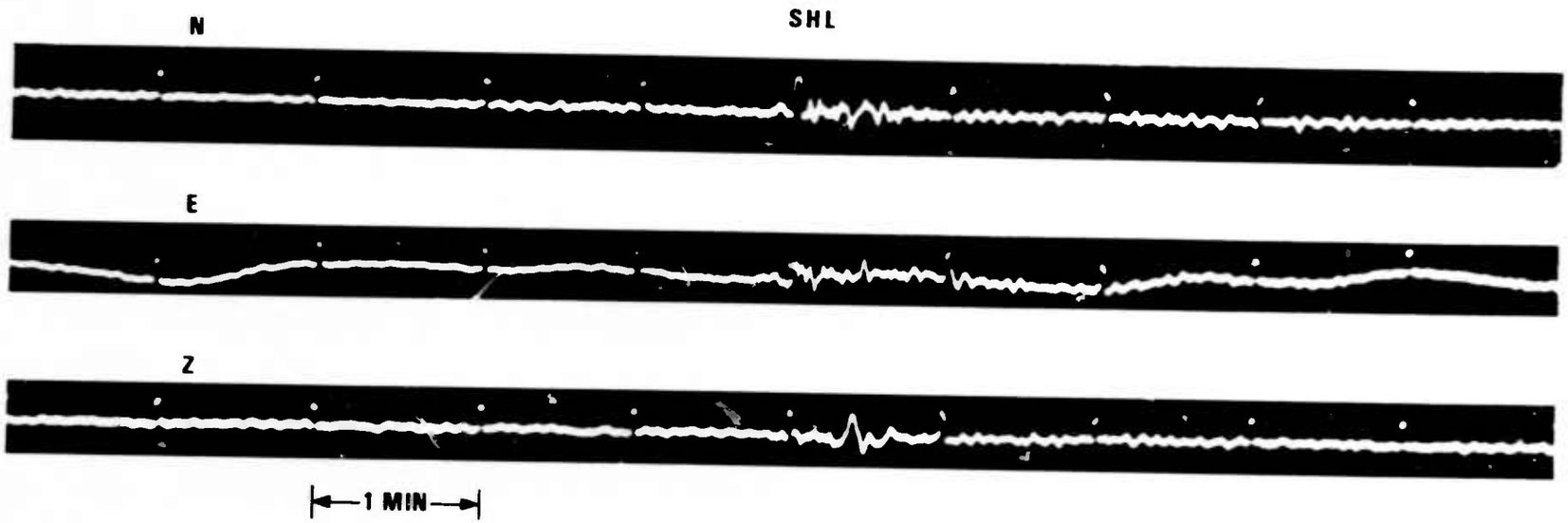

Figure 5. Long-period seismograms for the event on 7/19/68, 30.2°N 94.9°E, recorded at SHL.

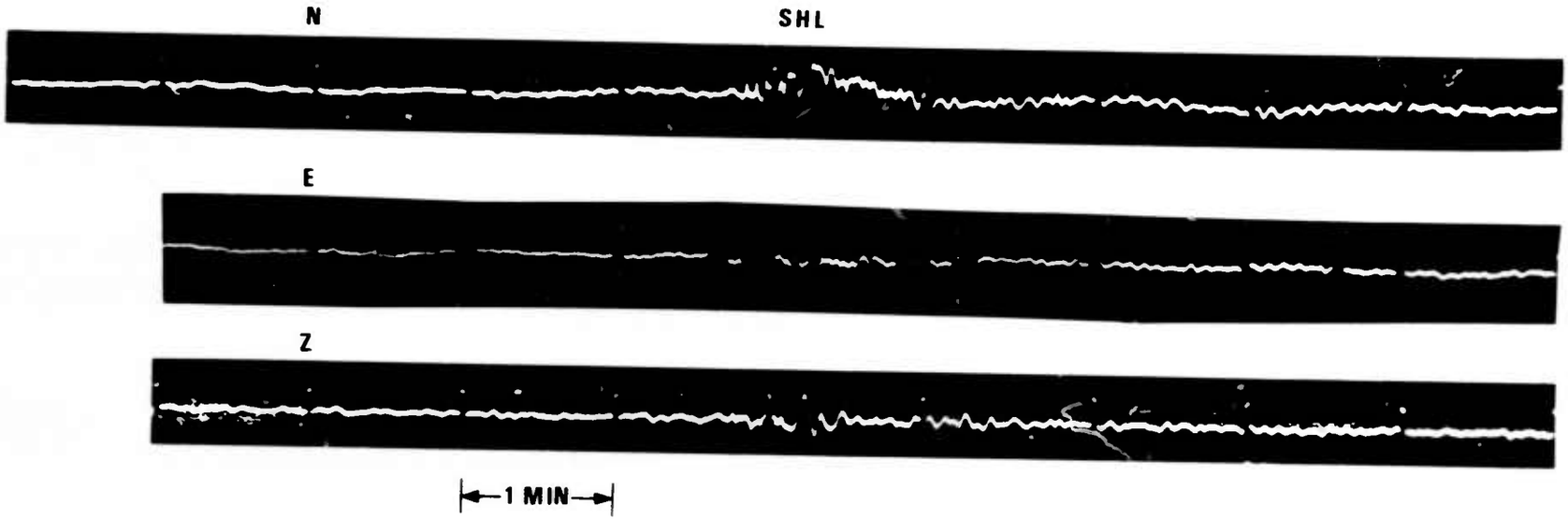

Figure 6. Long-period seismograms for the event on 7/26/68, 30.3°N 94.9°E, recorded at SHL.

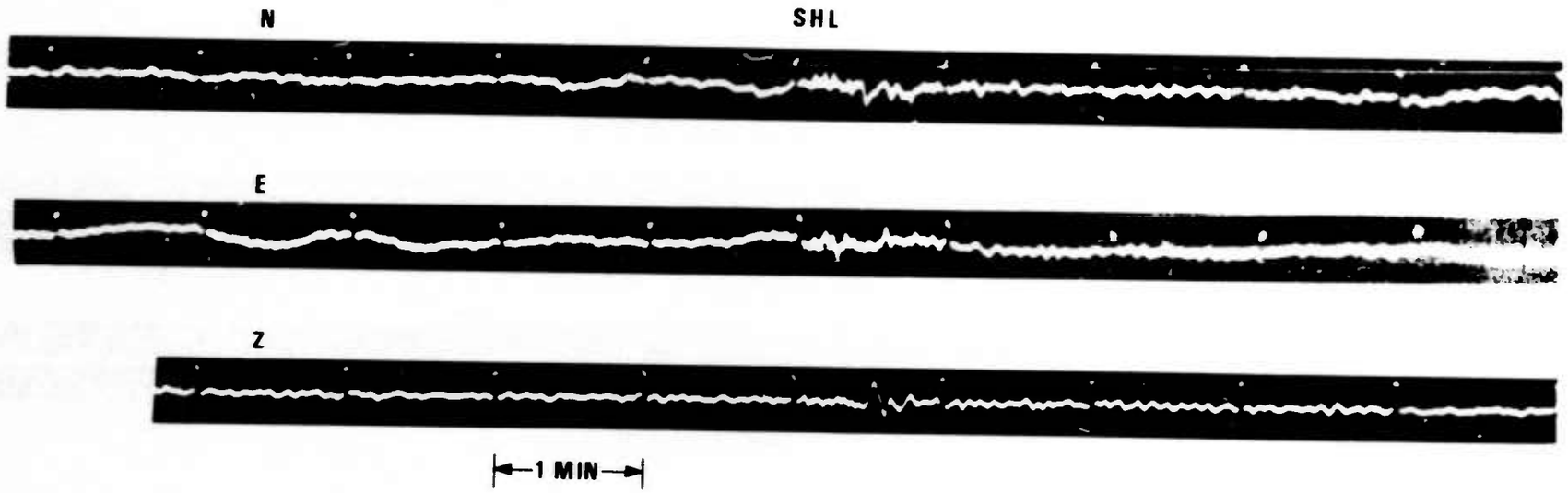

Figure 7. Long-period seismograms for the event on 7/26/68, 29.4°N 95.0°E, recorded at SHL.

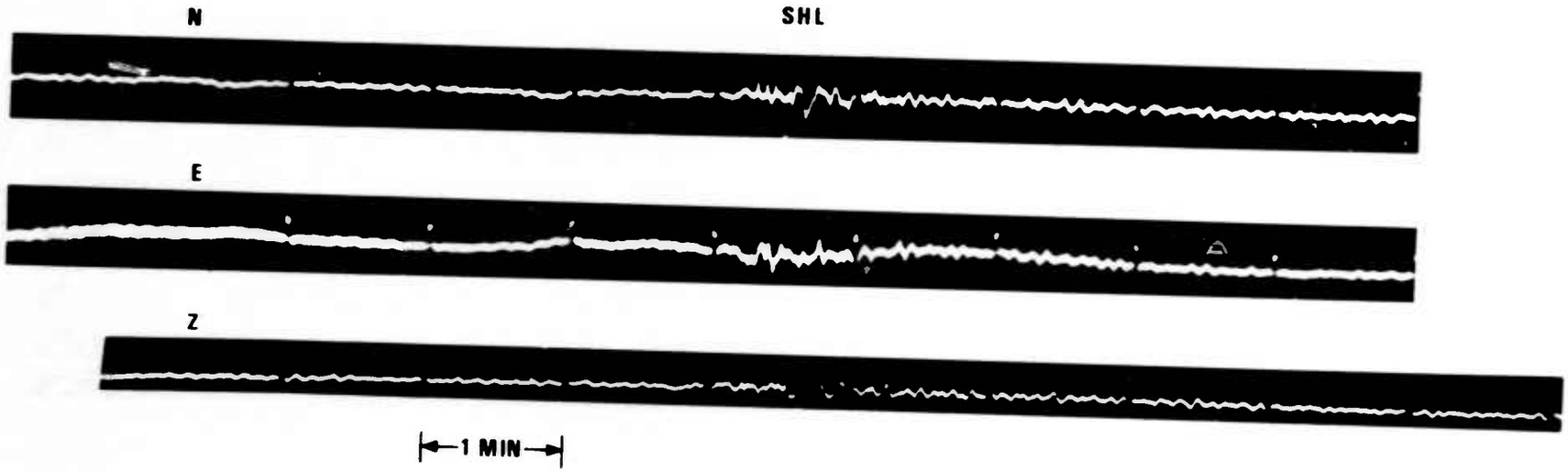

Figure 8. Long-period seismograms for the event on 8/23/68, 30.2° 94.9°E, recorded at SHL.

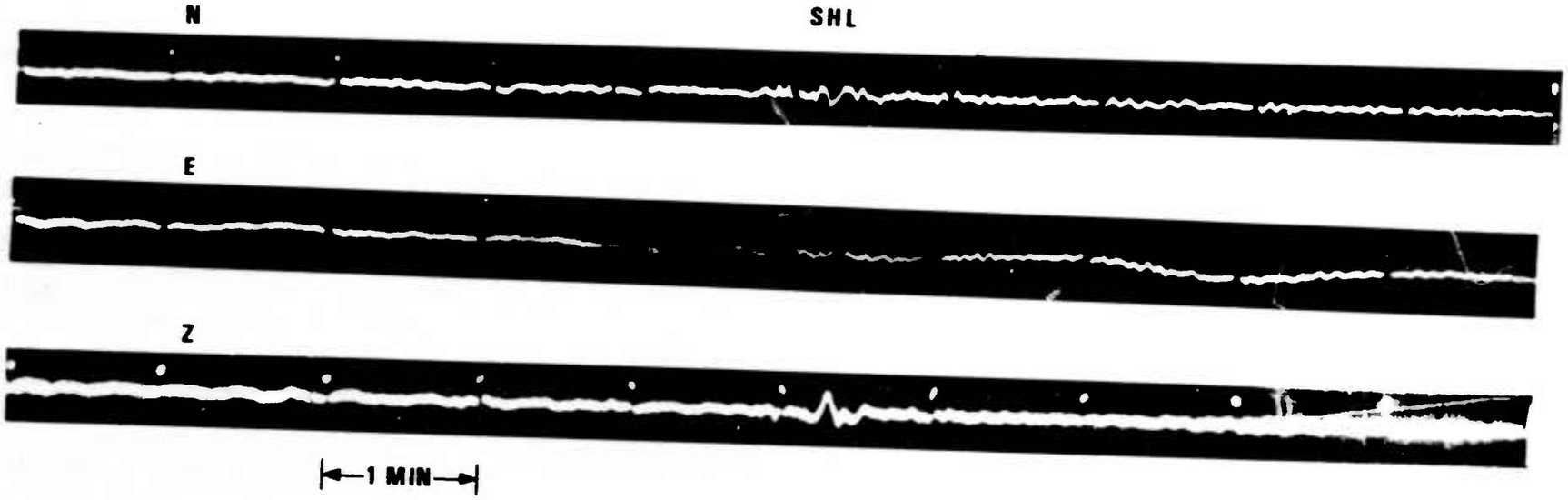

Figure 9. Long-period seismograms for the event on 9/03/68, 30.2°N 94.9°E, recorded at SHL.

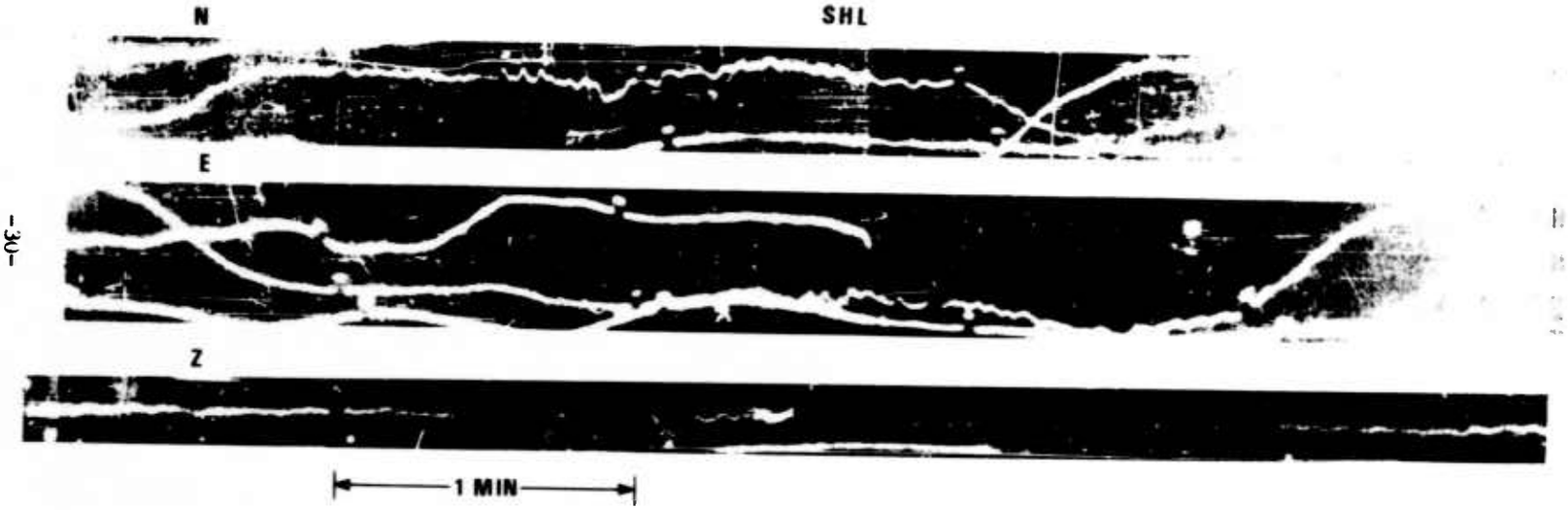

Figure 10. Long-period seismograms for the event on 10/06/64, 30.3°N 94.6°E, recorded at SHL.

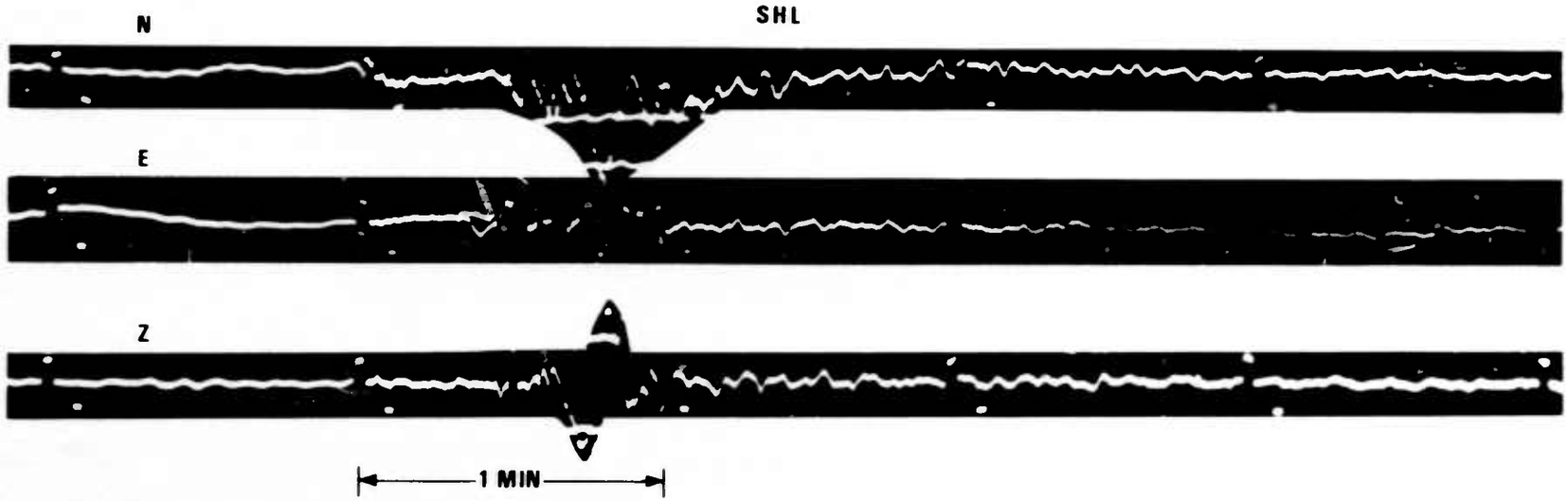

Figure 11. Long-period seismograms for the event on 7/05/66, 27.5°N 92.4°E, recorded at SHL.

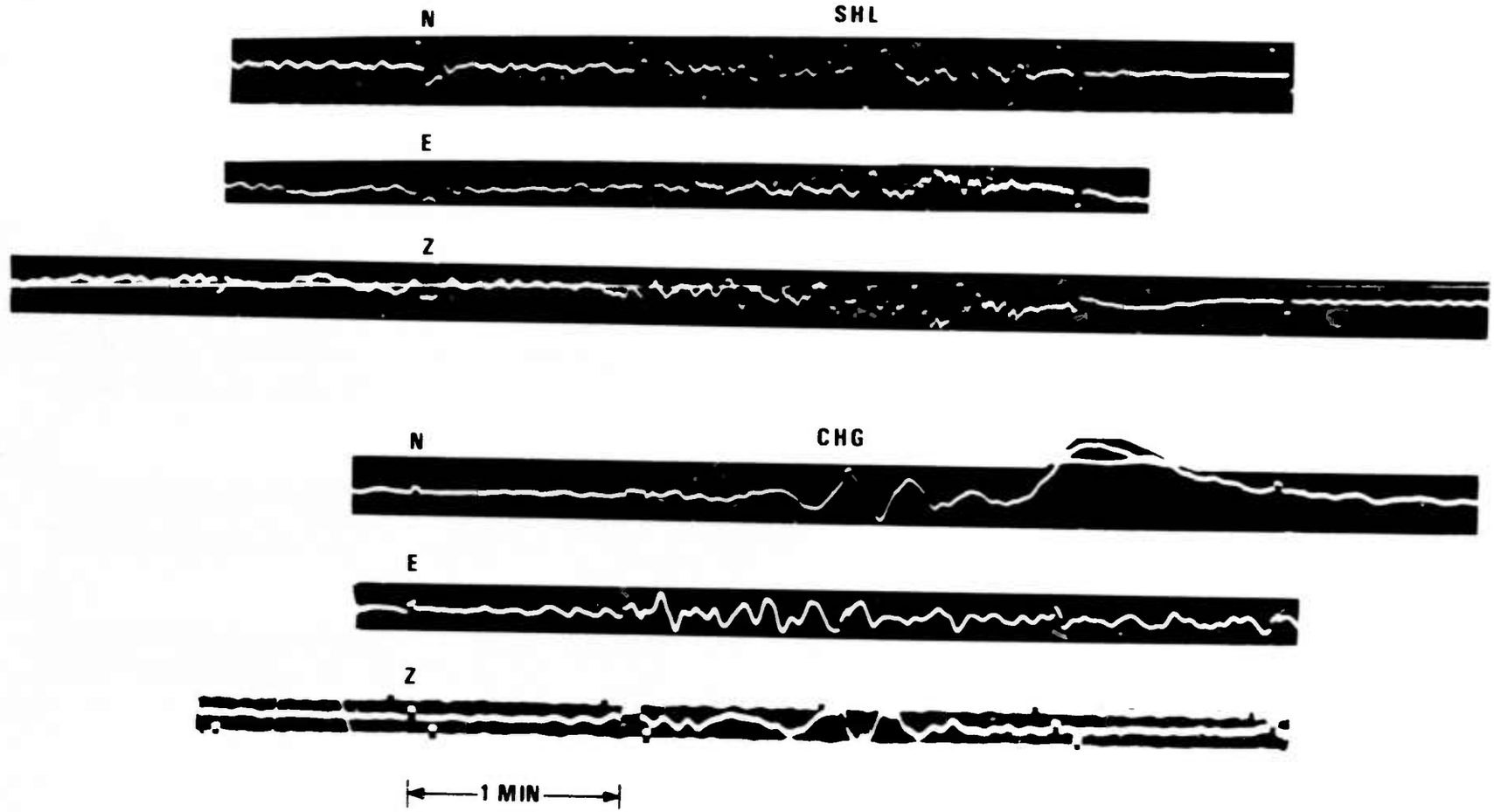

Figure 12. Long-period seismograms for the event on 9/11/66, 27.0°N 95.8°E, recorded at SHL and CHG.

At Chiang Mai no P or S is visible. Fundamental Rayleigh and Love waves are present, as well as indications of higher mode Rayleigh waves.

The recordings of the earthquake 9/26/66 at Shillong (Figure 13) again show long period P, S, and Rayleigh waves.

The recording of the event 7/07/67 shows S and Rayleigh waves (Figure 14).

Long-Period S to Long-Period Rayleigh Amplitude Ratios

Von Seggern (1972) and Blandford and Clark (1974) showed that the long-period S vs. Rayleigh wave amplitude ratio can be a good discriminant between earthquakes and explosions. Explosions generate long-period shear waves much less efficiently than earthquakes if the events are scaled to the same maximum Rayleigh amplitude. The data presented by von Seggern show that the mean of the logarithm of S/Rayleigh amplitude ratios is around -.3, corresponding to a ratio of about .5. Only the largest explosions generate visible long-period S waves. Since most of the events investigated in this report show at least indications of long-period S waves, this fact by itself place them in the earthquake population. Table VI shows the observed S to Rayleigh amplitude ratios at SHL. The values were obtained by measuring the periods and peak-to-peak amplitudes of the waves and correcting the latter for the instrument response. Rayleigh wave amplitudes were measured on the vertical component, S wave amplitudes on the horizontal components where the amplitude was maximum.

The value for the clustered events is based on some faint indications of long period S. The measurements are questionable and if real they represent a maximum value. The ratios fall within the earthquake region of von Seggern, although such ratios are rather crude discriminants in the absence of distance corrections.

Location and Depth Studies

Table VII shows the results of location and depth determination using the travel times in Table II and with no constraints on either depth or location. Most of the depths are moderate except events 1 and 9; some are negative.

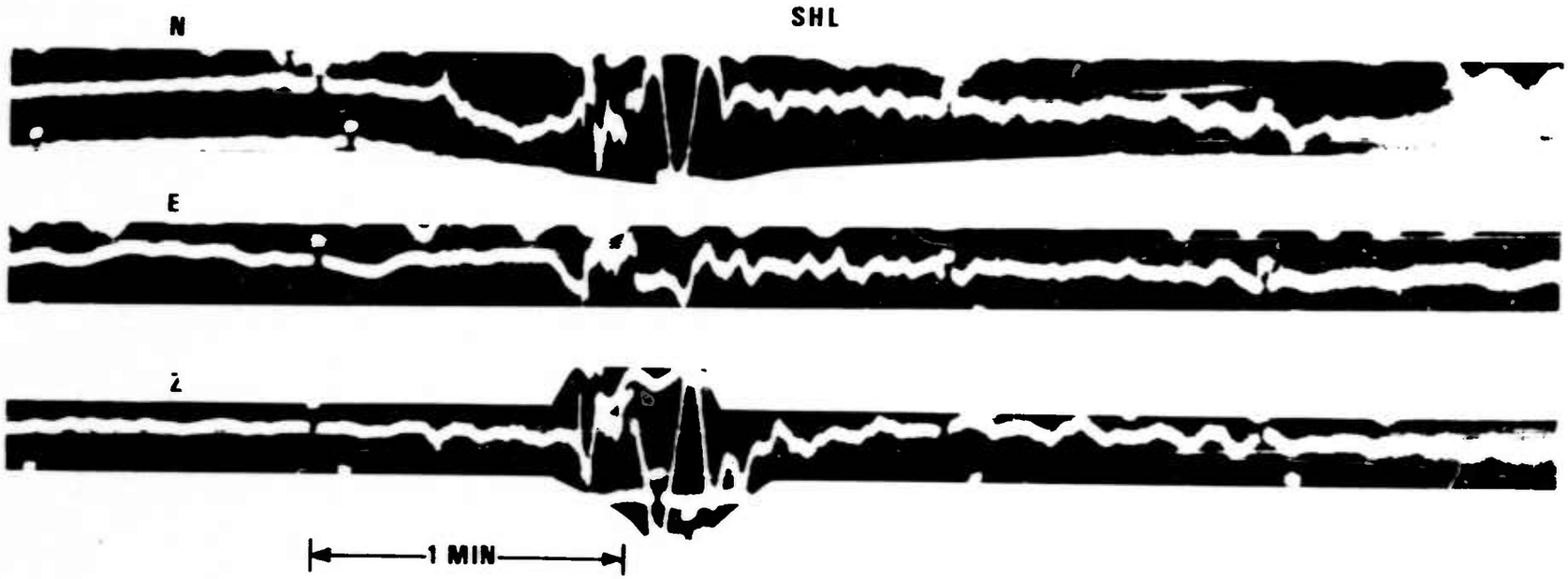

Figure 13. Long-period seismograms for the event on 9/26/66, 27.6°N 92.7°E, recorded at SHL.

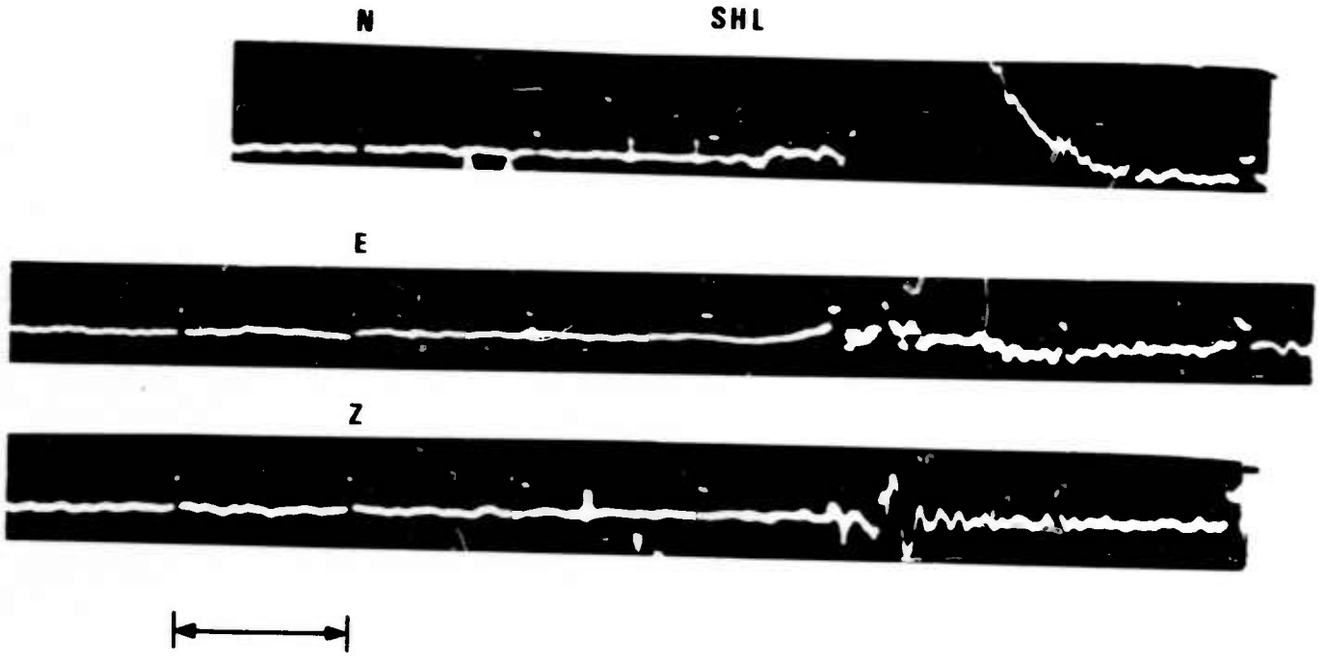

Figure 14. Long-period seismograms for the event on 7/07/67, 27.8°N 92.2°E, recorded at SHL.

TABLE VI

Long Period/Rayleigh Amplitude Ratios

Event	R (S/Rayleigh Amplitude Ratio)	Log R
10/06/64	.75 ?	-.12 ?
07/05/66	.25	-.61
07/07/66	.62	-.21
09/11/66	.60	-.23
09/26/66	.78	-.11
Cluster at 30°N, 95°E	~.84 ??	-.08 ??

TABLE VII

Relocation of Events Without Constraints

Date Mo	Day	Yr	Origin Time	Depth	SDV(R)	Shift KM	AZ
10	06	64	02:54:45.9	175	0.8	92	201
09	11	66	15:55:12.1	- 34	0.6	59	348
09	26	66	NO CONVERGENCE				
07	07	67	22:56:35.1	49	1.2	16	207
06	28	68	20:35:00.2	74	1.4	17	261
06	30	68	05:04:13.7	52	0.7	7	308
07	01	68	03:11:10.6	46	0.0	21	350
07	04	68	06:46:22.5	227	0.8	78	306
07	13	68	06:05:57.0	50	1.2	5	169
07	14	68	18:12:40.1	1	1.0	24	357
07	16	68	22:23:06.4	23	1.1	6	56
07	19	68	18:49:00.2	16	1.3	23	307
07	23	68	20:51:50.3	31	0.9	19	293
07	25	68	03:34:16.5	49	0.2	21	302
07	26	68	12:44:12.6	67	4.1	48	293
08	23	68	12:00:53.1	146	1.7	56	26
08	25	68	17:55:11.5	54	0.6	24	209
08	29	68	19:51:29.3	62	0.8	33	269
09	01	68	05:59:33.5	70	0.9	25	170
09	03	68	17:45:53.9	32	1.6	18	18
08	15	69	NO CONVERGENCE				

As the next step we tried to derive regional travel time anomalies by constraining the depths of events 13, 14, and 16 (which were recorded at many stations) to the NOS depths (which incidentally are within the range allowed by pP times) performing a location run, and considering the travel time residuals as travel time anomalies for the region surrounding these events. This is the SRST approach of Veith and Clawson (1973). The residuals for the three events showed some resemblance, so we took the averages for the three events as travel time anomalies. These are shown in Table VIII. Applying the residuals as travel time corrections to all events, we relocated the events. The results of the computations are shown in Table IX. There are no significant changes in the depths.

An attempt was also made to refine the location by means of an additional restraining of the origin time by use of S-P arrival time differentials. S-P times together with the standard JB tables determined a set of distance and corresponding P travel times. By subtracting the travel time from the arrival time, a origin time estimate is obtained. However, the resulting origin times deduced from different stations generally did not agree within an acceptable limit. The reason was probably in the difficulty of determining a good S start time for the distant stations. Since most events had readings from SHL and KBL, at distances of about 5° and 20° respectively, it was decided to use only these stations for estimating origin times.

A plot of the observed values of S-P vs. P time for those events with readings at both SHL and KBL (Figure 15), indicates that the average slope is about .83 as opposed to a slope of .78 from the JB tables within the same distance range. Therefore, a constant fraction, .83/.78, of the JB S-P versus O-P line was used to determine the origin time from readings at SHL and KBL for all events.

Based upon the new origin times, location runs were again made and the results are shown in Tables X and XI. As can be seen from the tables, the depths recalculated do not change appreciably. Some move deeper, some shallower in comparison to the previous runs, but with the exception of one event, they are all shallower than 100 kms.

TABLE VIII

Travel Time Anomalies (Residuals)

SHL	0.4
CHG	0.5
NDI	-0.9
KBL	1.3
QUE	-0.8
SHI	0.0
NUR	1.3
TRI	0.0
COL	-1.3
BUL	-0.9
POO	0.8
SEO	0.0
AAE	0.0
CTA	-0.4

TABLE IX

Relocation of Events with Travel Time Corrections using Residual

Mo	Date Day	Yr	Origin Time	Depth	SDV(R)	Shift KM	AZ
10	06	64	02:54:43.5	150	0.8	65	203
09	11	66	15:55:13.7	- 23	1.1	59	346
09	26	66	NO CONVERGENCE				
07	07	67	22:56:34.8	50	0.7	12	225
06	28	68	20:35:01.3	89	1.3	15	247
06	30	68	05:04:14.5	67	1.3	3	58
07	01	68	03:11:10.3	52	0.0	29	348
07	04	68	06:46:15.1	176	0.4	23	290
07	13	68	06:05:58.0	61	2.0	12	187
07	14	68	18:12:41.6	11	1.8	24	3
07	16	68	22:23:08.3	39	1.8	5	93
07	19	68	18:49:01.9	29	1.9	30	299
07	23	68	20:51:51.5	42	1.8	30	95
07	25	68	03:34:17.0	56	1.1	23	293
07	26	68	12:44:14.0	84	4.2	44	284
08	23	68	12:00:56.5	-122	2.0	51	26
08	25	68	17:55:12.7	69	1.4	32	207
08	29	68	19:51:30.1	72	1.4	34	262
09	01	68	05:59:33.3	75	0.8	19	160
08	15	69	17:45:52.7	23	1.9	25	24
			NO CONVERGENCE				

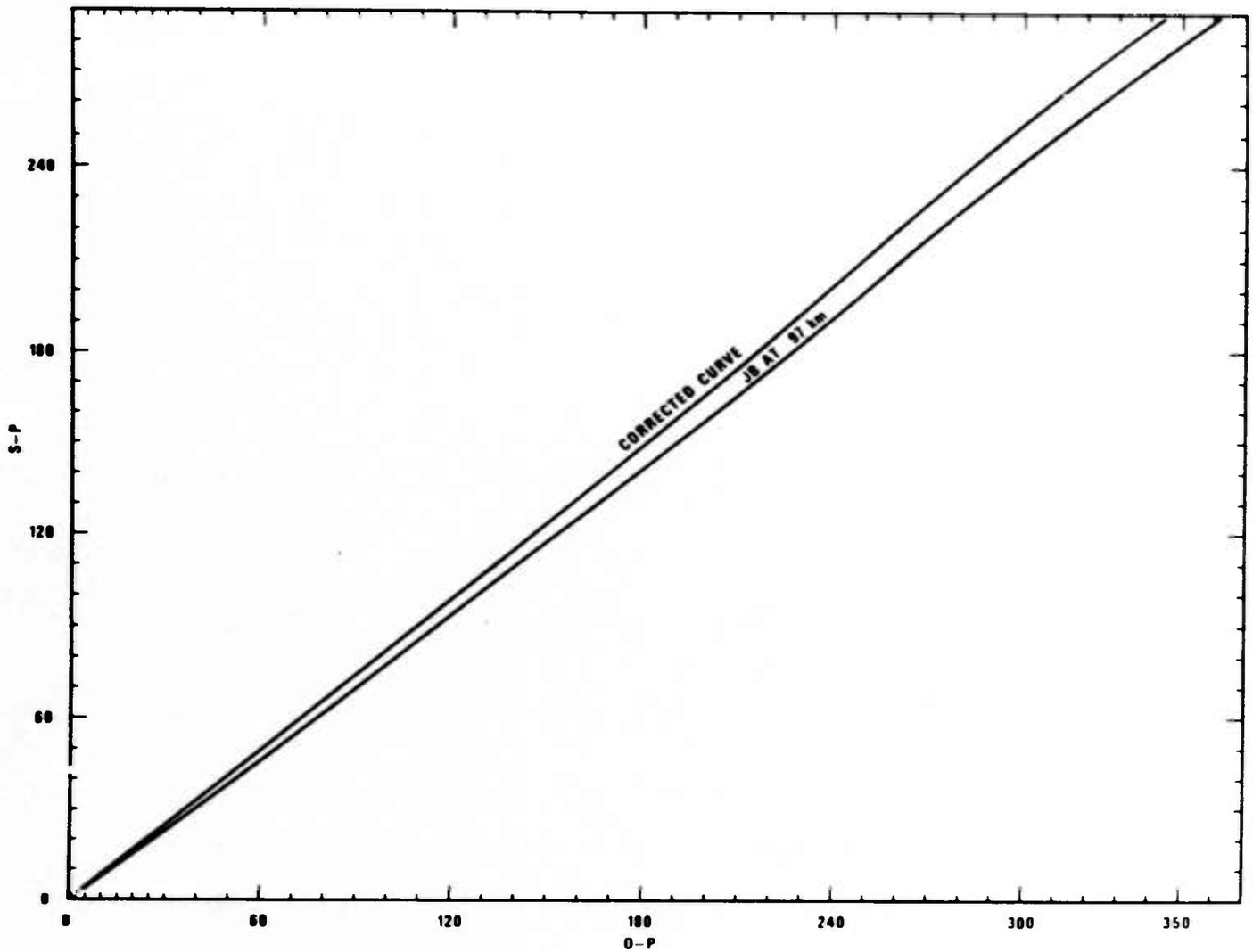

Figure 15. S-P travel time difference plotted against P travel times at SHL and KBL.

TABLE X

Relocation of Events with Origin Times Restrained

Date						Shift	
Mo	Day	Yr	Origin Time	Depth	SDV(R)	KM	AZ
10	06	64	N/A				
09	11	66	N/A				
09	26	66	N/A				
07	07	67	N/A				
06	28	68	20:35:01	82	1.4	21	249
06	30	68	05:04:14	55	0.7	7	291
07	01	68	03:11:19	126	2.2	42	186
07	04	68	06:46:04	68	1.1	18	306
07	13	68	06:06:00	79	1.3	24	209
07	14	68	18:12:48	66	1.9	21	267
07	16	68	22:23:13	83	1.5	33	207
07	19	68	18:49:08	84	1.8	43	239
07	23	68	20:51:55	76	1.3	36	239
07	25	68	N/A				
07	26	68	12:44:07	20	4.3	54	323
08	23	68	12:01:25	78	3.5	39	225
08	25	68	17:55:08	24	0.8	8	203
08	29	68	19:51:24	16	1.1	29	316
09	01	68	N/A				
09	03	68	17:46:00	91	2.0	20	218
08	15	69	07:15:46	56	3.5	76	293

TABLE XI

Relocation of Events with Origin Times
Restrained and Travel Time Corrections

Mo	Date Day	Yr	Origin Time	Depth	SDV(R)	Shift KM	AZ
10	06	64	N/A				
09	11	66	N/A				
09	26	66	N/A				
07	07	67	N/A				
06	28	68	20:35:01	87	1.3	14	252
06	30	68	05:04:14	62	1.3	6	40
07	01	68	03:11:19	135	2.3	37	191
07	04	68	06:46:04	82	0.6	14	153
07	13	68	06:06:00	81	2.0	24	199
07	16	68	18:12:48	65	2.1	12	268
07	16	68	22:23:13	85	2.0	31	202
07	19	68	18:49:08	86	2.2	41	239
07	23	68	20:51:55	77	1.9	30	238
07	25	68	N/A				
07	26	68	12:44:07	22	4.5	53	329
08	23	68	12:01:25	81	3.5	37	224
08	25	68	17:55:08	25	1.7	6	196
09	01	68	N/A				
09	03	68	17:46:00	91	2.3	16	216
08	15	69	07:15:46	62	4.2	92	299

RELATIVE LOCATION STUDIES

Although the exact epicentral location of the events studies do not have, in general, any bearing on the discrimination problem, knowledge of these locations could be helpful in relating the events to local tectonic patterns. Of special interest are the clustered events situated around 30°N and 95°E. These events are very similar in their characteristics and occur in a limited area. The epicentral locations given by NOS are given to an accuracy of .1° and are scattered over an area of 50 x 50 km. Using a different network for each event would result in a different network bias in location of each event. Thus even if all events occurred at the same point, their computed location would scatter over a wide area. By using common networks for several events it can be expected that their relative locations can be determined with higher accuracy, although the absolute locations could be wrong. Therefore the following approach was adopted. Common networks were chosen for pairs of events and the differences in latitude and longitude ($\Delta\lambda_{ij}$,$\Delta\phi_{ij}$) were computed for each pair. The values obtained naturally do not constitute an internally consistent set; therefore, the values are adjusted using least squares. However, this procedure is not quite correct, since the errors of the various $\Delta\lambda_{ij}$ and $\Delta\phi_{ij}$ are not independent, because they were computed by using overlapping sets of observing stations. The correct procedure to use is the joint epicenter determination method of Douglas (1967); see also Ahner, Blandford, and Shumway (1971) for which no working computer program is available at present at SDAC. Nevertheless the applied procedure should also remove the network biases and result in acceptable relative location provided that the travel time anomalies behave consistently over the area studies. The first attempt to use the method outlined above resulted in an average rms inconsistency of relative locations larger than .1°. This was judged to be too large, so combinations with large travel time residuals were discarded and the procedure repeated. The rms error decreased to .07° (which is still quite large) and the locations, although different from those given by NOS, did not seem to occupy an area of different size. The relative locations of the same events are shown in Figure 16a, together with locations by NOS in Figure 16b. Both depth and epicenter calculations thus show that discrepancies

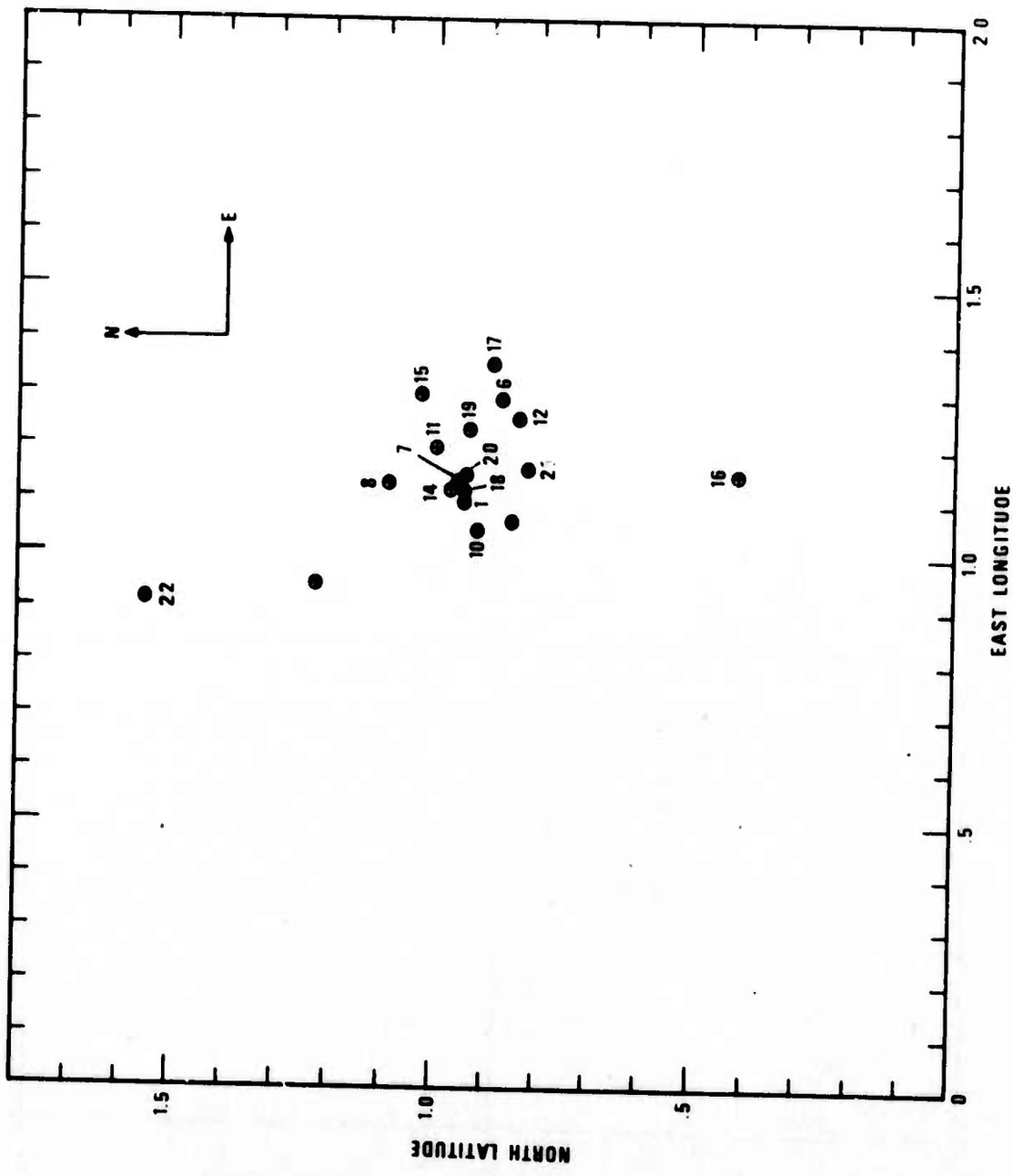

Figure 16a. Recomputed locations of events around 30°N-95°E.

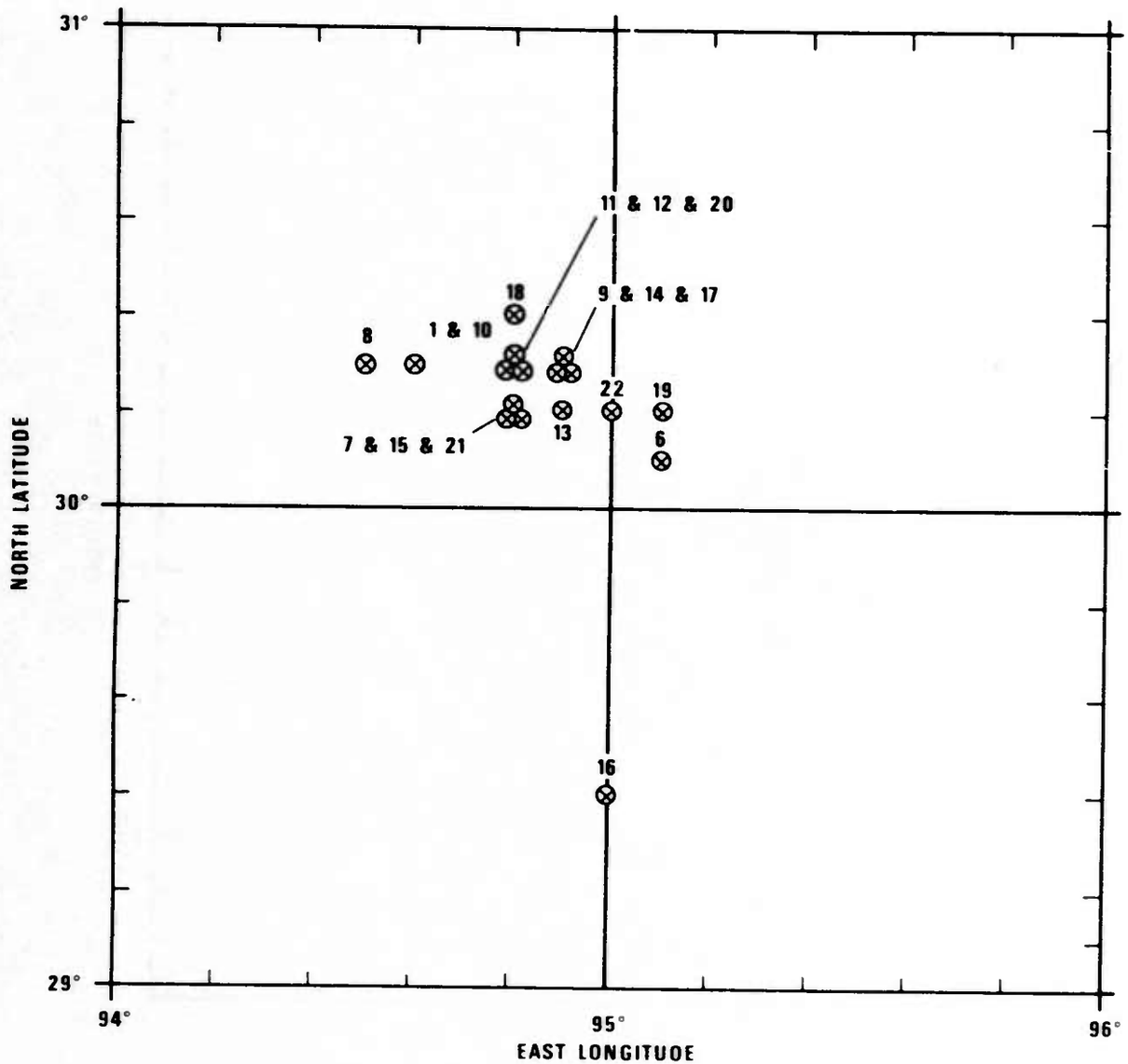

Figure 16b. NOS locations of events around 30°N-95°E.

are present in the travel time readings and the travel time anomalies which prevent more accurate determination of depths and epicenters. The only positive statement that can be made is that the events do not occupy a wider area than originally supposed, and there are no indication that they are confined to a considerably smaller area, a narrow fault trace, say. Since event 2 (in Table I) had only 3 P readings it was omitted from the calculations.

Summarizing the recomputation of event locations and depths, it can be concluded that all attempts to refine locations and depths were defeated by poor data quality and no significant and demonstrable improvement was achieved. The calculations indicate, however, that there is no reason to believe the events studied are considerably deeper than the depths given by NOS, so it is unlikely that the low M_s values are due to great source depths.

M_s-m_b Values

Body wave magnitudes were recomputed incorporating data at teleseismic stations. The additional magnitude values computed are given in Table XII. The magnitudes derived with station corrections from Report #296 (Der, 1973) were combined with m_b determinations at the teleseismic stations. We did not attempt to derive station corrections for the teleseismic stations. The m_b values at the additional stations agreed well with the values of m_b at the network used in Report #296, which eliminates the possibility that there were relatively high m_b values due to network bias at near stations. The new m_b values differ little from those given in Report #296. The M_s values remain unchanged, since the addition of new stations did not result in more surface wave detections. The new M_s and m_b values are given in Table I. The depth correction .008h used in Report #296 and based on NOS depth was removed from the M_s values in this table, since in our opinion the body-wave data are not of sufficient quality to rule out the possibility that these events are deep. If then the events are possibly shallow, then application of this correction begs the question.

Marshall and Basham (1972) derived their depths from amplitude measurements of the dispersed surface wave train at various dominant periods. This was not possible in our case since most of the surface wave observed were short transients which could not be analyzed without digitization and Fourier analysis. The quality of the available photographic records was poor and it was not practical to digitize them. Besides, calculations by von Seggern

TABLE XII

Body-Wave Magnitudes (m_b)
at Teleseismic Stations

Event Date	Station	m_b	Event Date	Station	m_b
64/10/06	COL	4.67	68/07/19	BUL	4.90
	BUL	4.48		COL	4.85
	SHI	4.47		NUR	4.91
66/09/11	BUL	4.14		SHI	4.53
	COL	4.03	68/07/23	BUI	4.96
	SHI	4.30		COL	4.78
66/09/26	CTA	4.48		NUR	4.83
	COL	4.59		SHI	4.61
	BUL	4.29	68/07/25	BUL	4.90
67/07/07	BUL	4.76		COL	4.98
	COL	4.89		NUR	4.94
	CTA	4.48		SHI	4.78
	SHI	5.01	68/07/26	BUL	4.96
68/06/28	BUL	4.62		COL	4.82
	COL	4.93		NUR	4.80
	CTA	4.90		SHI	4.58
	SHI	4.62		TRI	4.91
	TRI	5.17	68/08/23	BUL	4.66
68/06/30	BUL	4.68		COL	4.92
	COL	4.79		NUR	4.94
68/07/01	COL	4.42	68/08/25	BUL	4.88
	TRI	4.90		COL	4.85
68/07/04	BUL	4.84		CTA	4.66
	COL	4.85		NUR	4.67
	NUR	4.83	68/08/29	BUL	4.68
	SHI	4.78		COL	4.92
68/07/13	COL	4.87		NUR	5.04
	SHI	4.67		SHI	4.64
68/07/14	BUL	4.94	68/09/01	BUL	4.50
	SHI	4.79		COL	4.85
	COL	4.98		SHI	4.60
	NUR	4.87	68/09/03	COL	4.82
	TRI	5.26		CTA	4.88
68/07/16	BUL	4.83		NUR	4.91
	COL	4.92	69/08/15	BUL	4.91
	NUR	5.08		COL	5.09
	SHI	4.49		SHI	4.78

using Harkrider's theory of surface wave generation showed that the method used by Marshall and Basham to determine depth is extremely unreliable. Thus the separation of earthquakes and explosions achieved by Marshall and Basham must be partially due to spectral differences between earthquakes and explosions. Without the "depth correction" the separation of explosion and earthquake is less pronounced, and low M_s earthquakes are liable to be mistaken for explosions.

This problem is especially severe for relatively small events where the surface waves can be seen only at nearby stations at low signal-to-noise ratios. This is precisely the case we are dealing with. Without the depth correction most of the events studied here seem to have an anomalously low M_s compared to m_b, and could potentially be mistaken for explosions if the M_s-m_b discriminant is used.

Effect of Abnormally Thick Crust on Surface Waves

The source region studied is anomalous in its crustal thickness. Estimates of crustal thickness from surface wave studies are in the range 70-90 km (Gupta and Narain 1967). The anomalously thick crust presumably results from the underthrusting of the Indian subcontinent under Eurasia. To ascertain that the low surface wave excitation is not due to abnormally thick crust we have calculated the surface wave excitation factor A_R (Harkrider, 1964).

From Harkrider (1964) and from equations (12) and (24) in Ben-Menahem and Harkrider (1964) one may derive the equation

$$A_{LR} = M(\omega) A_R \left(\frac{\omega}{C_R}\right)^{1/2} \left(\frac{W_s}{W_o}\right) \chi(\Theta)$$

where $M(\omega)$ is the source strength ($M(o)$ = moment), C_R is the Rayleigh phase velocity, and W_s/W_o is the ratio of model amplitudes at source depth. Note that W_s/W_o is unity for surface sources, and greater at any depth in a thick crust than in a shallow one because the fundamental mode amplitude decays more slowly if the velocity increases slowly with depth. C_R decreases as the crust increases in thickness and von Seggern (1971) has shown that A_R is proportional to $(UC_R)^{-1}$ (where U is the group velocity) which also would be expected to increase in a thick crust. Thus one would expect that the effect of a 70-90 km

crust would be to increase M_s if measured on the thick crust, not to decrease it. And in fact explicit calculations give increases of .2 to .4 M_s units over a Gutenberg crust.

Now let us suppose that the amplitude measurement takes place on thin crust and that the wave has crossed via a smooth transition. It seems plausible that the amplitude would revert to what it would have been for a source in the thin crust. In fact, McGarr (1969) obtains theoretically and experimentally a shift of magnitude not significantly different from $U^{-3/2}$ for an ocean continent transition. Thus for measurement on a thin crust, we would expect the net effect to approximately vanish. Note that this failure to explain low surface waves by a completely elastic mechanism does not rule out the low Q proposed by Lambert (1974) as an explanation.

The dominant period of Rayleigh waves observed is 10-15 sec which indicates that most events considered are shallow since greater source depth would drastically decrease the amplitude of these waves relative to the longer periods which we do not observe.

SEARCH FOR ADDITIONAL ANOMALOUS EVENTS

Search for low (M_s-m_b) events was performed in a wider area around the region previously studied. All NOS events occurring between 25-45°N and 68-100°E in the time interval June 4, 1968, and September 30, 1972 were used, except for those already discussed in SDL 296, and those which had no m_b listed by NOS. The time interval given was determined by the availability of the data from the WWSSN station Kabul (KBL), Afganistan. This station operates at very high magnifications on both the short-period and long-period instruments. It is located inside the region searched, and is therefore quite suitable for detecting the events to be studied. It can be expected that the single-station m_b values would be unreliable since path and station effects for short-period P waves can result in standard deviations of the order of .5 magnitude units. Single-station M_s values have a smaller scatter due to path and station effects but can be influenced by radiation patterns. In view of these factors, the following strategy was adopted: m_b values as listed by NOS were used (which were presumably computed by averaging m_b values of several stations) jointly with M_s values determined at KBL alone. Previous experience, Der (1973), showed that m_b values given by NOS are in general higher than these determined by SDAC. Too-high m_b values would minimize the chance of missing some truly anomalous events. Similarly some M_s values will be too low at KBL due to radiation patterns. These events, if truly normal in their M_s-m_b characteristics, can be eliminated later after closer examination. Thus the combination of NOS m_b and KBL stations M_s values can be used to sift through the initial data set and eliminate most events with normal M_s-m_b values. Table XIII gives the events in the initial data set with the M_s and m_b values used. Events which are not given here but listed by NOS were eliminated because of undetectable signal amplitudes, some operational difficulty at KBL, or interference with other events. It is of course possible that some of the events eliminated because no LR was detectable were truly the events we were looking for. The M_s values were computed by Marshall and Basham's method using depth corrections with depth taken from NOS. Figure 17 shows the plot of M_s-m_b values obtained. In all, 165 M_s-m_b pairs are shown. The

TABLE XIII

Body and Surface Wave Magnitudes at KBL

Date	Event Origin Time	Latitude	Longitude	Depth	NOS m_b	m_b	M_s Prague	M_s M&B	M_s DVS
68/06/10	17:36:30.0	39.0N	75.1E	51	4.8	5.16	3.84	4.18	4.35
68/06/14	04:02:22.0	31.2N	70.2E	25	4.9	-	3.60	5.29	4.24
68/07/01	19:14:54.7	44.0N	79.3E	33	4.9	4.63	3.08	3.53	3.45
68/07/20	08:22:08.6	39.4N	73.8E	61	4.8	4.89	3.73	3.94	4.26
68/07/26	20:48:03.2	32.1N	70.1E	35	4.8	-	3.60	4.39	4.31
68/08/09	02:24:53.2	25.2N	94.4E	34	4.7	-	3.24	3.56	3.47
68/08/18	14:18:59.5	26.4N	90.6E	31	5.2	-	3.97	4.26	4.24
68/09/12	15:36:48.8	39.8N	77.8E	8	4.9	-	4.41	4.21	4.86
68/10/10	22:49:01.5	37.2N	70.0E	34	4.9	-	3.18	3.82	3.88
68/10/28	17:48:29.1	27.3N	86.1E	37	4.8	3.97	3.59	3.63	3.93
68/11/01	20:49:17.3	37.6N	72.2E	41	4.7	-	3.08	3.17	3.71
68/11/05	02:02:44.2	32.4N	76.4E	33	4.9	-	3.45	4.20	3.97
68/12/08	15:51:59.0	41.6N	70.1E	33	4.8	4.84	3.93	3.88	4.39
69/01/05	02:38:51.8	39.9N	75.8E	33	4.8	-	3.46	3.85	3.94
69/01/05	09:56:41.1	28.0N	85.2E	33	-	3.49	3.39	3.26	3.72
69/01/05	18:51:23.3	26.6N	96.7E	53	-	-	3.97	3.97	4.19
69/01/23	20:01:19.5	32.2N	76.1E	33	4.0	4.47	2.96	3.02	3.49
69/01/23	23:46:26.0	32.2N	76.0E	33	-	4.72	2.51	3.22	3.04
69/02/12	00:22:37.4	41.3N	79.3E	33	4.9	5.36	4.18	4.19	4.59
69/02/12	04:17:19.4	41.5N	79.5E	33	4.7	4.92	3.66	3.58	4.07
69/02/15	23:59:10.6	41.5N	79.5E	33	5.0	5.33	3.95	4.26	4.36
69/02/18	19:51:27.5	29.7N	68.4E	51	4.6	-	3.41	4.45	3.99
69/02/22	20:37:07.1	26.6N	92.4E	52	4.8	5.22	3.66	3.99	3.92
69/03/01	15:00:20.0	41.4N	79.4E	33	4.6	-	2.88	3.38	3.29
69/03/03	06:20:21.8	30.2N	79.9E	20	5.3	-	3.87	4.17	4.29
69/03/03	14:03:00.5	31.0N	71.8E	33	4.5	-	3.55	3.65	4.16
69/03/11	19:20:28.1	41.3N	79.5E	33	4.7	5.01	3.41	3.73	3.81
69/03/27	11:19:29.3	39.0N	71.9E	37	4.9	-	3.51	3.75	4.08
69/03/27	19:37:44.1	39.0N	71.8E	33	5.2	-	3.41	3.79	3.98
69/04/03	02:52:50.9	41.2N	79.2E	40	4.5	5.00	3.72	3.96	4.13

TABLE XIII (Continued)

Body and Surface Wave Magnitudes at KBL

Date	Event Origin Time	Latitude	Longitude	Depth	NOS m_b	m_b	M_s Prague	M_s M&B	M_s DVS
69/04/25	07:36:36.2	30.8N	70.3E	23	4.9	-	3.60	4.37	4.22
69/04/28	12:50:15.2	25.9N	95.3E	50	5.2	-	3.64	3.72	3.87
69/05/01	04:00:08.7	44.0N	77.9E	53	4.9	5.38	-	-	-
69/05/04	13:48:33.6	41.5N	86.7E	32	4.7	4.79	3.93	3.86	4.25
69/05/13	10:04:38.6	39.9N	70.9E	33	4.8	-	3.38	3.54	3.92
69/06/01	08:35:22.1	25.8N	91.8E	20	5.0	-	3.56	3.57	3.81
69/06/04	00:39:57.5	41.4N	79.5E	33	4.9	5.43	3.72	4.04	4.12
69/06/09	18:52:26.3	42.0N	84.6E	36	4.7	4.12	3.26	3.67	3.60
69/06/21	17:32:56.6	35.6N	81.9E	33	4.5	4.97	3.63	3.81	4.04
69/06/22	01:33:24.1	30.6N	79.4E	19	5.4	-	4.08	4.33	4.51
69/06/25	04:42:40.6	41.4N	79.4E	35	4.8	4.72	3.46	3.65	3.87
69/06/29	03:40:12.9	41.1N	75.8E	39	5.1	4.77	3.24	3.69	3.69
69/07/18	13:10:31.9	43.3N	97.0E	33	4.6	4.51	3.79	4.05	4.02
69/07/20	04:34:14.9	39.8N	77.8E	33	5.0	5.61	4.30	4.39	4.75
69/08/27	22:35:53.6	35.4N	71.4E	55	5.2	-	3.57	3.94	4.34
69/08/28	04:06:21.9	39.2N	73.9E	26	5.1	-	4.03	4.43	4.56
69/09/16	21:19:26.5	39.8N	75.1E	19	4.9	5.35	3.90	3.87	4.39
69/09/20	04:48:45.5	29.7N	68.6E	40	5.2	-	4.18	4.54	4.76
69/09/20	14:07:57.8	38.4N	69.8E	52	5.1	-	3.28	4.39	3.91
69/09/22	16:14:58.8	41.4N	88.3E	-	5.1	-	3.31	3.12	3.62
69/09/23	12:31:55.0	30.3N	69.6E	30	4.5	4.79	3.74	4.12	4.34
69/09/27	16:56:25.2	38.6N	75.1E	33	4.9	-	4.08	4.13	4.60
69/09/30	23:13:28.8	25.6N	94.7E	20	5.4	4.36	3.82	3.51	4.05
69/12/05	18:45:17.4	29.7N	80.8E	33	4.9	5.18	3.42	3.49	3.81
69/12/09	13:41:09.0	40.1N	70.7E	33	5.0	-	2.96	3.80	3.51
69/12/29	18:08:55.8	37.0N	71.8E	42	4.7	-	3.08	3.65	3.74
70/01/09	21:00:09.9	43.0N	80.5E	33	4.9	-	2.99	3.91	3.37
70/01/19	00:31:52.6	41.1N	69.3E	43	5.0	-	3.49	4.20	4.00
70/01/19	12:57:28.4	27.0N	97.0E	45	4.6	-	3.87	4.43	4.10
70/01/19	23:04:40.3	40.6N	74.2E	47	4.6	-	3.54	3.81	4.03
70/01/23	12:02:08.5	32.4N	87.9E	33	4.6	4.55	3.89	3.65	4.21
70/02/08	10:12:42.2	39.7N	73.7E	45	5.2	-	3.24	3.63	3.76
70/02/12	01:51:51.4	29.4N	81.6E	44	5.4	-	3.96	4.32	4.34

TABLE XIII (Continued)

Body and Surface Wave Magnitudes at KBL

Date	Event Origin Time	Latitude	Longitude	Depth	NOS m_b	m_b	M_s Prague	M_s M&B	M_s DVS
70/02/22	06:56:20.4	37.1N	72.0E	33	4.7	-	2.52	2.76	3.17
70/03/05	18:34:22.5	32.4N	76.5E	33	4.9	-	3.09	3.88	3.60
70/03/12	14:36:56.7	42.2N	72.3E	42	5.2	4.63	3.16	3.66	3.63
70/03/16	03:47:06.4	33.9N	86.3E	52	4.9	4.68	3.58	3.63	3.92
70/03/24	15:45:57.8	36.1N	68.8E	54	4.8	-	3.30	3.99	4.11
70/03/29	03:48:47.3	39.6N	75.4E	33	5.1	-	3.89	4.60	4.38
70/04/15	05:45:20.1	39.0N	70.7E	33	4.6	-	3.12	3.27	3.71
70/04/19	05:33:46.2	39.0N	70.8E	33	4.7	-	2.76	3.15	3.35
70/04/19	08:49:37.3	38.8N	75.3E	33	4.8	-	2.91	3.48	3.42
70/04/24	03:29:12.9	38.4N	69.0E	31	4.6	-	3.65	4.00	4.28
70/04/28	18:43:15.8	38.9N	70.9E	41	5.0	-	2.70	3.38	3.29
70/04/30	03:24:54.8	33.1N	73.4E	39	5.0	-	3.83	4.09	4.46
70/06/08	07:05:55.4	36.2N	68.8E	47	4.8	-	3.38	4.11	4.20
70/06/12	16:00:01.4	40.7N	78.4E	33	5.0	-	3.71	3.84	4.14
70/06/19	15:08:49.6	38.8N	70.7E	33	4.5	4.67	2.98	3.39	3.58
70/07/25	01:35:26.3	25.7N	88.5E	33	5.2	-	4.30	4.68	4.58
70/07/26	20:30:35.5	34.8N	73.2E	33	5.1	-	3.44	3.84	4.09
70/08/06	05:44:14.2	40.4N	78.8E	33	4.5	5.20	3.51	3.73	3.94
70/08/09	16:12:17.4	40.0N	77.8E	33	4.5	-	3.37	3.69	3.82
70/08/11	01:06:19.3	34.1N	79.3E	33	4.8	5.12	3.59	3.86	4.05
70/09/11	02:42:20.9	29.9N	70.4E	20	4.9	-	3.20	3.40	3.78
70/09/14	09:49:33.5	39.9N	77.0E	33	5.2	-	4.76	5.03	5.22
70/09/18	20:02:25.0	36.4N	68.9E	33	5.1	-	2.71	3.82	3.50
70/10/05	10:42:49.1	40.1N	77.1E	33	5.0	-	3.79	4.13	4.24
70/10/09	13:48:52.6	39.1N	71.7E	46	5.2	-	3.23	4.44	3.80
70/10/14	00:36:34.5	31.2N	74.3E	33	5.2	-	2.66	3.22	3.21
70/10/14	07:29:58.6	40.9N	89.4E	-	4.6	3.65	4.47	4.92	4.77
70/10/15	03:55:16.1	39.8N	77.2E	33	4.9	-	4.34	4.36	4.80
70/10/15	04:42:19.0	39.8N	77.2E	33	4.6	-	3.75	3.94	4.21
70/11/16	04:57:32.9	43.2N	81.2E	24	5.2	5.03	4.32	4.96	4.69
70/11/29	02:03:37.4	41.6N	81.8E	33	5.1	5.42	3.91	4.11	4.29
70/11/29	15:31:29.7	41.6N	81.8E	33	4.7	5.47	3.96	4.29	4.33
70/12/01	22:45:04.7	41.7N	81.7E	33	-	4.82	3.11	3.50	3.49
70/12/08	11:53:16.2	38.9N	70.4E	33	-	4.33	2.95	3.71	3.55
70/12/08	22:50:47.3	38.9N	70.3E	59	4.4	4.64	3.04	3.93	3.63

TABLE XIII (Continued)

Body and Surface Wave Magnitudes at KBL

Date	Event Origin Time	Latitude	Longitude	Depth	NOS m_b	m_b	M_s Prague	M_s M&B	M_s DVS
70/12/30	09:35:25.8	40.3N	72.7E	33	5.0	4.82	3.43	3.87	3.94
71/01/04	19:01:20.3	29.2N	69.2E	33	4.9	-	4.55	4.98	5.10
71/01/08	23:52:16.3	29.1N	69.1E	4	5.2	-	4.26	4.53	4.82
71/01/30	20:15:40.8	30.5N	79.1E	56	4.6	5.16	2.83	3.61	3.26
71/02/01	14:21:42.9	43.0N	85.3E	33	4.8	4.58	3.02	3.55	3.35
71/02/05	09:10:35.7	25.2N	99.4E	33	5.3	5.54	4.89	5.16	4.89
71/02/21	11:45:24.8	40.8N	72.6E	33	4.2	4.94	3.76	5.01	4.26
71/03/01	00:56:51.5	34.1N	95.8E	33	4.6	4.36	3.67	3.95	3.92
71/03/11	23:59:46.5	40.1N	77.1E	33	-	5.41	3.61	4.20	4.06
71/03/15	22:57:17.6	32.9N	68.1E	41	4.3	-	4.33	4.63	5.12
71/03/24	13:54:17.7	35.5N	98.2E	13	5.8	-	5.56	5.88	5.79
71/03/24	20:54:28.6	41.5N	79.5E	18	5.3	5.71	4.31	4.57	4.72
71/03/24	21:01:54.9	41.4N	79.4E	25	5.3	-	4.51	4.83	4.92
71/03/31	08:16:19.6	26.2N	96.6E	22	5.0	5.15	3.95	3.99	3.95
71/03/31	20:00:31.5	39.6N	74.8E	38	4.8	4.82	4.31	4.44	4.81
71/04/06	03:02:57.0	39.6N	77.8E	33	4.5	-	3.74	3.83	4.19
71/04/18	07:24:14.3	39.1N	71.7E	33	4.5	-	3.29	3.50	3.86
71/04/21	09:15:22.9	26.6N	92.2E	33	4.3	4.11	3.63	3.87	3.88
71/04/21	14:39:53.1	41.5N	79.2E	40	5.1	5.01	3.24	3.69	3.65
71/04/27	14:47:55.2	39.2N	72.9E	37	4.8	4.13	4.27	4.23	4.82
71/05/03	00:33:22.5	30.8N	84.5E	16	5.4	-	5.12	5.07	5.47
71/05/14	17:14:40.9	25.1N	68.1E	57	4.5	5.36	3.46	4.14	3.89
71/05/27	00:30:27.7	38.3N	69.0E	36	4.8	4.35	3.38	3.85	4.01
71/05/30	11:55:59.9	25.3N	96.4E	33	4.9	-	4.65	4.78	4.65
71/05/30	21:39:00.5	25.3N	96.4E	33	4.9	5.24	4.26	4.26	4.26
71/06/04	20:49:58.3	32.2N	92.1E	33	5.0	4.17	4.19	3.88	4.47
71/06/06	10:34:49.0	28.1N	85.6E	34	4.9	4.37	3.90	3.44	4.22
71/06/15	07:39:37.1	41.4N	79.4E	33	5.6	-	4.85	5.10	5.25
71/06/15	22:04:13.4	41.5N	79.3E	33	5.6	5.73	-	-	-
71/06/15	22:15:49.7	41.4N	79.3E	33	5.1	5.81	4.50	4.51	4.91
71/06/15	23:17:33.9	41.6N	79.2E	33	4.9	-	3.70	4.02	4.11
71/06/16	00:58:37.4	41.5N	79.4E	33	5.4	-	4.82	5.00	5.23
71/06/16	10:56:38.7	41.4N	79.3E	33	5.0	5.51	3.68	4.06	4.09
71/06/16	13:46:50.5	41.3N	79.3E	33	5.1	5.53	3.90	4.29	4.31
71/06/17	15:20:12.0	41.3N	79.4E	33	5.2	5.44	3.49	3.67	3.90
71/06/19	17:23:02.7	41.5N	79.3E	33	5.2	5.68	4.88	5.13	5.29

TABLE XIII (Continued)

Body and Surface Wave Magnitudes at KBL

Date	Event Origin Time	Latitude	Longitude	Depth	NOS m_b	m_b	M_s Prague	M_s M&B	M_s DVS
71/06/19	21:08:45.8	41.5N	79.4E	33	4.7	5.30	3.54	3.54	3.94
71/06/22	10:25:32.9	41.3N	79.3E	47	4.8	5.09	3.29	3.66	3.70
71/07/01	14:37:25.7	36.7N	68.3E	33	4.6	-	3.48	3.74	4.22
71/07/03	04:26:22.1	41.3N	79.3E	17	4.9	5.11	-	-	-
71/07/17	15:00:55.4	26.5N	93.2E	49	5.3	-	4.80	5.31	5.05
71/07/24	11:43:38.8	39.5N	73.2E	33	5.6	4.84	4.12	4.66	4.66
71/07/30	20:13:14.1	41.3N	79.3E	33	4.5	5.34	3.77	3.79	4.19
71/08/07	15:21:52.5	36.1N	77.7E	33	4.8	-	4.21	4.55	4.71
71/08/09	01:03:16.6	42.1N	83.4E	33	4.2	-	3.33	3.68	3.68
71/08/29	15:16:56.9	36.5N	78.5E	33	5.0	-	2.78	3.81	3.25
71/09/21	09:13:51.5	32.3N	91.8E	33	5.0	-	4.39	4.54	4.67
71/09/25	08:53:20.9	37.8N	69.7E	56	4.5	3.86	3.21	3.57	3.87
71/10/01	16:27:47.7	38.6N	69.8E	36	4.9	-	4.23	4.36	4.84
71/10/24	08:59:04.6	28.3N	87.2E	44	5.1	-	3.68	3.27	3.99
71/10/28	13:30:57.1	41.8N	72.4E	22	5.5	-	4.94	5.08	5.42
71/10/29	17:16:52.1	34.1N	86.3E	33	5.0	5.59	4.01	4.07	4.35
71/10/31	15:54:47.9	26.2N	90.7E	33	4.6	4.79	3.49	3.56	3.76
71/11/19	01:00:01.0	41.9N	72.4E	33	4.9	-	4.38	4.37	4.86
71/11/24	08:23:24.6	38.7N	73.3E	33	5.1	-	2.86	3.04	3.42
71/12/04	08:38:00.7	27.9N	87.9E	32	5.0	-	3.23	3.53	3.53
71/12/12	13:41:39.8	41.4N	79.2E	33	4.7	4.90	3.52	3.62	3.93
71/12/12	22:27:41.1	39.5N	73.2E	33	4.8	-	3.60	3.67	4.13
71/12/27	20:59:34.1	35.1N	73.1E	10	5.4	-	3.65	3.97	4.31
71/12/29	22:27:02.2	25.1N	94.7E	33	5.5	-	4.49	5.10	4.72
71/12/30	23:35:27.6	39.8N	77.5E	33	4.9	-	3.87	3.97	4.32

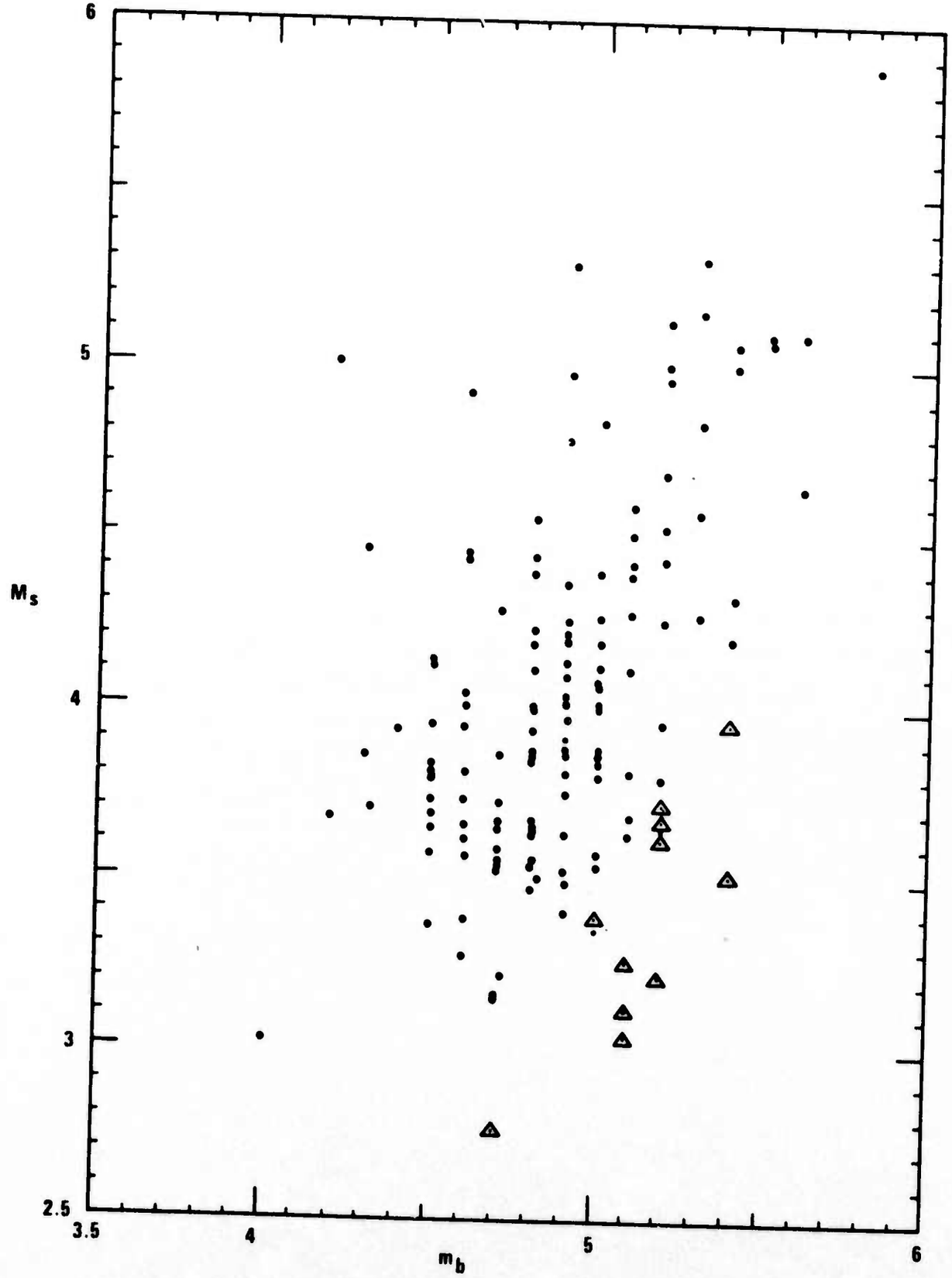

Figure 17. M_s-m_b data for the events in an extended area between 24-45° and 68-100°E. M_s values were computed at KBL. m_b values are those of NOS. Triangles are the events further investigated.

line $M_s = 1.38m_b - 3.45$ was used as the dividing line between "anomalous" and normal events; it lies midway between the earthquake and explosion lines of Marshall and Basham (1972). Eleven points lie below the line (the events in question are marked in Table XIII by a star). One of them, the event in Sinkiang, is a presumed explosion.

To investigate these eleven events further, film chips were ordered from NOS for the stations NUR, TRI, SHI, POO, SHL, QUE, BUL, AAE, CTA, COL, NDI in addition to KBL. P wave and Rayleigh wave amplitudes were read and magnitudes computed. The recomputed magnitudes are shown in Table XIV and are plotted against Marshall and Basham's 95% confidence limits for earthquakes and explosions in Figure 18. The filled circles in this figure are the M_s-m_b pairs. The figure shows that only two of the points lie close to the 95% confidence limit of Eurasian explosions; one of these points is an explosion. The remaining points are close to the 95% line for earthquakes. Since there is a considerable uncertainity in determining these lines, it is not clear that anything is unusual, since the number of "anomalous" points is about 5% of the total events considered. Thus the population searched is not much different from that presented by Marshall and Basham. The most anomalous earthquake is located in the Tadzhik SSSR, but the point is based on only three m_b and one M_s reading.

TABLE XIV
Body and Surface Wave Magnitudes for Events
which appear to be anomalous at KBL

Event Date	Origin Time	Latitude	Longitude	Depth	NOS m_b	Station	m_b	M_s Prague	M&B	DVS
71/12/27	20:59:34.1	35.1N	73.1E	10	5.4	CHG	4.56	-	-	-
						NUR	5.13	-	-	-
						QUE	5.80	3.67	4.09	4.17
						KBL	-	3.65	3.97	4.31
						Average	5.16	3.66	4.03	4.24
71/10/24	08:59:04.6	28.3N	87.2E	44	5.1	CHG	4.10	-	-	-
						COL	4.89	-	-	-
						NUR	5.24	-	-	-
						QUE	4.16	-	-	-
						KBL	-	3.68	3.27	3.99
						Average	4.60	3.68	3.27	3.99
71/06/17	15:20:12.0	41.3N	79.4E	33	5.2	COL	4.99	-	-	-
						NDI	4.71	-	-	-
						NUR	4.99	-	-	-
						QUE	4.62	3.17	3.70	3.51
						KBL	5.44	3.49	3.67	3.90
						Average	4.95	3.33	3.69	3.70
70/10/14	00:36:34.5	31.2N	74.3E	33	5.2	NDI	-	2.81	3.70	3.46
						POO	5.39	3.60	3.85	3.97
						QUE	5.24	2.95	3.81	3.47
						SHL	4.23	3.02	3.72	3.34
						KBL	--	2.66	3.22	3.21
						Average	4.96	3.01	3.66	3.49
70/04/28	18:43:15.8	38.9N	70.9E	41	5.0	BUL	5.10	-	-	-
						COL	4.90	-	-	-
						NDI	5.79	3.79	4.12	4.09
						POO	3.55	4.13	4.17	4.44
						QUE	5.41	3.35	3.65	3.79
						KBL	-	2.70	3.38	3.29
						Average	4.95	3.48	3.83	3.90

TABLE XIV (Continued)
Body and Surface Wave Magnitudes for Events
which appear to be anomalous at KBL

Date	Event Origin Time	Latitude	Longitude	Depth	NOS m_b	Station	m_b	M_s Prague	M_s M&B	DVS
70/02/22	06:56:20.4	37.1N	72.0E	33	4.7	NDI	5.15	-	-	-
						NUR	4.21	-	-	-
						SHL	4.51	-	-	-
						KBL	-	2.52	2.76	3.17
						Average	4.62	2.52	2.76	3.17
70/02/08	10:12:42.2	39.7N	73.7E	45	5.2	BUL	5.06	-	-	-
						CHG	-	4.13	4.42	4.13
						COL	4.84	-	-	-
						NDI	5.72	3.90	4.45	4.31
						NUR	4.97	-	-	-
						POO	4.24	4.02	4.25	4.29
						KBL	-	3.24	3.63	3.76
						Average	4.97	3.82	4.19	4.12
69/09/30	23:13:28.8	25.6N	94.7E	20	5.4	BUL	5.04	-	-	-
						NDI	4.50	3.90	3.95	4.21
						POO	4.44	-	-	-
						QUE	5.49	3.92	3.82	4.14
						SHI	-	4.93	4.52	5.15
						KBL	4.36	3.82	3.51	4.05
						Average	4.77	4.14	3.95	4.39
69/09/22	16:14:58.8	41.4N	88.3E	-	5.1	CHG	4.68	-	-	-
						COL	5.57	-	-	-
						NDI	5.03	-	-	-
						POO	5.41	-	-	-
						QUE	4.69	3.72	3.52	3.98
						SHL	4.15	-	-	-
						KBL	-	3.31	3.12	3.62
						Average	4.92	3.16	3.32	3.80
69/04/28	12:50:15.2	25.9N	95.3E	50	5.2	BUL	4.86	4.98	5.36	4.98
						TRI	6.00	-	-	-
						SHL	-	3.55	4.20	4.22
						COL	5.16	-	-	-
						NUR	5.69	-	-	-
						POO	4.19	3.80	4.12	4.06
						QUE	5.34	3.86	4.18	3.86
						KBL	-	3.64	3.72	3.87
						Average	5.21	3.97	4.14	4.20

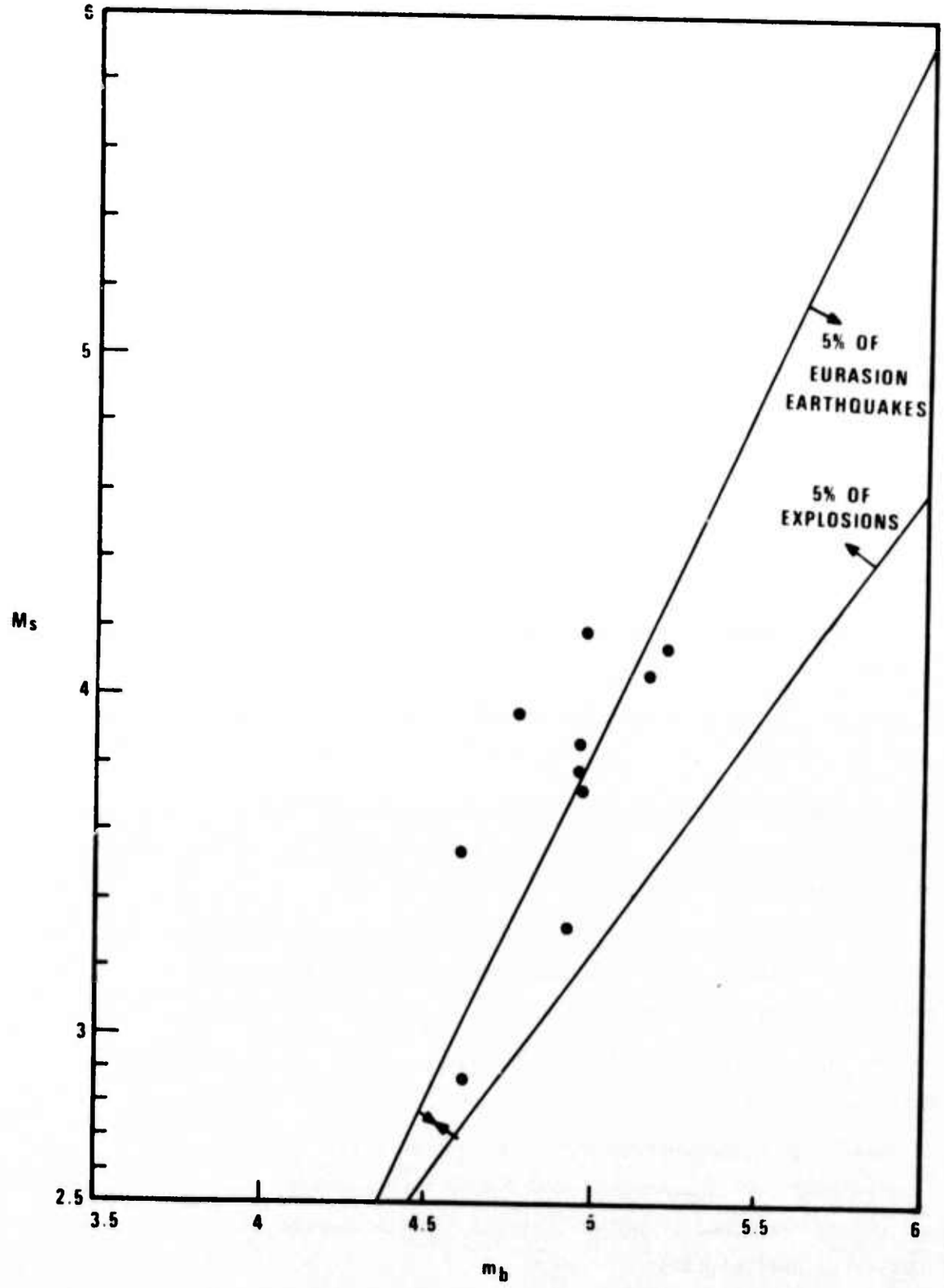

Figure 18. Revised M_s-m_b values of apparently anomalous events in the extended area. 95% confidence limits of earthquake and explosion populations marked (after Marshall and Basham, 1972).

SUMMARY AND CONCLUSIONS

The analysis of low M_s events in the Himalayan region using an expanded network gave the following conclusions:

1. The M_s values are confirmed to be relatively low compared to m_b values. Additional P-wave teleseismic readings did not change the m_b values appreciably.

2. Clear dilatations were observed at for many events, indicating that they are earthquakes rather than explosions.

3. Depth and location calculations using various constraints and a common network failed to provide refinement in the source location or depth due to the poor quality and internal inconsistencies of data. The calculations indicate, however, that most of the events are shallower than 80 km.

4. pP readings at teleseismic stations, although doubtful, also indicate that most of the events are shallow or normal in depth.

5. The long period S to Rayleigh amplitude ratios classify the events as earthquakes.

6. Anomalously thick crust in the source region is not likely to cause the low M_s values.

7. The event cluster centered at 30°N latitude and 95°E longitude consists of many similar events with almost identical long period seismograms. Love waves, if present, are unclear.

8. Three events on the Himalayan front show long-period S, two long-period P and two Love waves. The long period S to Rayleigh amplitude ratio is characteristic of earthquakes.

9. The short-period S to P ratio, where available, is characteristic of earthquakes.

10. Search for additional anomalous events in a wider area did not indicate any additional contiguous areas where such events occur. The low M_s events found can be explained by normal scatter of data and amount to a few percent of the total data studied.

The above results suggest that even low (M_s-m_b) events such as those discussed by Der (1973) can be shown to be earthquakes by careful analysis of the short-period data from close-in stations. Long-period shear to Rayleigh amplitude ratios seem also to classify them as earthquakes. The data quality is poor enough, however, that a fully satisfying discussion of the events is impossible. In particular we remain uncertain about the cause of the low (M_s-m_b) values; and we cannot be certain that the long-period shear wave discriminants are completely reliable because the measurements were made at distances of only 5° for which distance there are no data in the discrimination data bases of von Seggern (1972) or of Blandford and Clark (1974). Even if such data were available it would have to be carefully analyzed from a theoretical point of view to ensure that the unusually thick crust in Tibet does not bias the results. These remarks point out possible subjects for future research, which should become possible with the aid of high-quality data from the expanded VELA network.

REFERENCES

Ahner, R. O., R. R. Blandford, and R. H. Shumway, 1971, Applications of the joint epicenter determination method, SDL Report 275, Teledyne Geotech, AD 750769.

Ben-Menahem, A., and D. Harkrider, 1964, Radiation patterns of seismic surface waves from buried dipolar point sources in a flat shatified earth, J. Geophys. Res., 69, 2605-2620.

Blandford, R. R. and D. M. Clark, 1974, Detection of long-period S from earthquakes and explosions at LASA and LRSM stations with applications to positive and negative discrimination, SDAC-TR-75-15, Teledyne Geotech, Alexandria, Virginia.

Chiburis, E. F., 1968a, LASA travel-time anomalies for 65 regions computed with the Herrin travel-time table, November 1966 version: Seismic Data Laboratory Report No. 204, Teledyne Geotech, Alexandria, Virginia. AD 825280.

Chiburis, E. F., 1968b, Precision location of underground nuclear explosions using teleseismic networks and predetermined travel-time anomalies: Seismic Data Laboratory Report No. 214, Teledyne Geotech, Alexandria, Virginia. AD 832961.

Chiburis, E. F. and R. O. Ahner, 1970, A seismic location study of station anomalies, network effects, and regional bias at the Nevada Test Site: Seismic Data Laboratory Report No. 253, Teledyne Geotech, Alexandria, Virginia. AD 876477.

Chiburis, E. F., R. O. Ahner, and T. R. Potts, 1971, A location study of central Alaska earthquakes: Seismic Data Laboratory Report No. 274, Teledyne Geotech, Alexandria, Virginia. AD 886279.

Der, Z. A., 1973, M_s-m_b characteristics of earthquakes in the Eastern Himalayan regions: Seismic Data Laboratory Report No. 29o, Teledyne Geotech, Alexandria, Virginia. AD 759835.

Douglas, A., 1967, Joint epicenter determination, Nature, 220, p. 469.

Gupta, H. K. and H. Narain, 1967, Crustal structure in the Himalayan and Tibet plateau region from surface wave dispersion, Bull. Seism. Soc. Amer., v. 57, p. 235-248.

REFERENCES (Continued)

Harkrider, D., 1964, Surface waves in multilayered elastic media I. Rayleigh and Love waves from buried sources in a multilayered elastic halfspace, Bull. Seism. Soc. Amer., v. 54, p. 627-679.

Herrin, E. and J. Taggert, 1968, Source bias in epicenter determinations, Bull. Seism. Soc. Amer., v. 58, p. 1791-1796.

Isacks, B., J. Oliver, and L. R. Sykes, 1968, Seismology and new global tectonics, J. Geophys. Res., 73, p. 5855-5899.

Lambert, D., 1974, Observed Rayleigh wave group velocities and spectral amplitudes for some Eurasian paths, Texas Instruments Technical Report No. 1, ALEX(01)-TR-74-01, Alexandria, Virginia.

LePichon, X., 1968, Sea floor spreading and continental drift, J. Geophys. Res., 73, p. 3661-3697.

Marshall, P. D. and P. W. Basham, 1972, Discrimination between earthquakes and underground explosions employing an improved M_s scale. geophys., J. R. Astr. Soc., 28, p. 431-458.

McGarr, A., 1972, Propagation of Rayleigh waves across a continental margin, Bull. Seism. Soc. Amer., v. 59, p. 1281-1306.

Veith, K. F. and G. E. Clawson, 1972, Magnitude from short period P-wave data, Bull. Seism. Soc. Amer., v. 62, p. 435-452.

von Seggern, D., 1971, Effects of propagation paths on surface-wave magnitude estimates, Seismic Data Laboratory Report 279, Teledyne Geotech, Alexandria, Virginia.

von Seggern, D. H., 1972, Seismic shear waves as a discriminant between earthquakes and underground nuclear explosions, Seismic Data Laboratory Report No. 295, Teledyne Geotech, Alexandria, Virginia. AD 747763.